

1 **Low spatial structure and selection against secreted virulence factors attenuates**
2 **pathogenicity in *Pseudomonas aeruginosa***

3

4 **Running title:** Virulence evolution in an opportunistic pathogen

5

6 Elisa T. Granato^{1,2}, Christoph Ziegenhain^{3,4}, Rasmus L. Marvig⁵, Rolf Kümmerli¹

7 ¹Department of Plant and Microbial Biology, University of Zurich, Zurich, Switzerland.

8 ²Department of Zoology, University of Oxford, Oxford, United Kingdom.

9 ³Department Biology II, Ludwig-Maximilians-University, Munich, Germany.

10 ⁴Department of Cell and Molecular Biology, Karolinska Institutet, Solna, Sweden.

11 ⁵Center for Genomic Medicine, Rigshospitalet, Copenhagen, Denmark.

12

13 **Corresponding author:** Dr. Elisa Granato

14 **Postal Address:**

15 Department of Zoology, University of Oxford

16 New Radcliffe House, Radcliffe Observatory Quarter

17 Woodstock Road, Oxford OX2 6GG

18 United Kingdom

19 **Email:** elisa.granato@zoo.ox.ac.uk

20 **Phone:** +44 1865 613338

21 **Competing Interests**

22 The authors declare no competing financial interests.

23 **ABSTRACT**

24 Bacterial opportunistic pathogens are feared for their difficult-to-treat nosocomial infections and
25 for causing morbidity in immunocompromised patients. Here, we study how such a versatile
26 opportunist, *Pseudomonas aeruginosa*, adapts to conditions inside and outside its model host
27 *Caenorhabditis elegans*, and use phenotypic and genotypic screens to identify the mechanistic
28 basis of virulence evolution. We found that virulence significantly dropped in unstructured
29 environments both in the presence and absence of the host, but remained unchanged in spatially
30 structured environments. Reduction of virulence was either driven by a substantial decline in the
31 production of siderophores (in treatments without hosts) or toxins and proteases (in treatments
32 with hosts). Whole-genome sequencing of evolved clones revealed positive selection and parallel
33 evolution across replicates, and showed an accumulation of mutations in regulator genes
34 controlling virulence factor expression. Our study identifies the spatial structure of the non-host
35 environment as a key driver of virulence evolution in an opportunistic pathogen.

36 INTRODUCTION

37 Understanding how microbial pathogens evolve is essential to predict their epidemiological
38 spread through host populations and the damage they can inflict on host individuals.
39 Evolutionary theory offers a number of concepts aiming at forecasting the evolution of pathogen
40 virulence and identifying the key factors driving virulence evolution [1,2]. While most
41 evolutionary models agree that the spatial structure of the environment is an important
42 determinant of virulence evolution, they differ on whether spatial structure should boost or curb
43 pathogen virulence. One set of models predicts that high spatial structure lowers virulence,
44 because it favors clonal infections and thereby limits the risk of hosts being infected by multiple
45 competing pathogen lineages [3–6]. In this scenario, it is thought that the interests of pathogens
46 in clonal infections become aligned, which should select for prudent host exploitation and thus
47 low virulence [7,8]. Another set of models predicts that high spatial structure increases virulence
48 because it favors the cooperative secretion of harmful virulence factors required for successful
49 host colonization [5,9,10]. These models are based on the idea that virulence factors, such as
50 toxins, proteases and iron-scavenging siderophores, are shared between pathogen individuals in
51 infections [11–13]. Hence, low spatial structure is predicted to favor the evolution of cheating
52 mutants that exploit the virulence factors produced by others, without contributing themselves
53 [14]. Invasions of these cheats would then lower overall virulence factor availability and damage
54 to the host [15–19].

55

56 Both classes of models have received some empirical support. While experimental evolution
57 studies with viruses showed that limited dispersal indeed favors more benign pathogens [20–22],
58 work with bacteria showed evidence for the opposite pattern [17,23,24]. Although these studies

59 significantly advanced our understanding of virulence evolution, several fundamental questions
60 remain still open. For instance, we generally know little about the mechanistic basis of virulence
61 evolution [8,20,21,25]. Moreover, bacterial studies often built on controlled mixed versus mono-
62 infections using wildtype strains and engineered mutants deficient for virulence factor
63 production [17,23,24]. It thus remains unknown whether virulence-factor deficient mutants
64 would indeed evolve *de novo* and spread to high frequency. Finally, we have limited
65 understanding of how adaptation to the non-host environment affects virulence evolution
66 [26,27], since most studies on bacterial opportunistic pathogens involved direct host-to-host
67 transfers [28–30].

68

69 Here we aim to tackle these unaddressed issues by conducting an experimental evolution study,
70 where we (i) allow opportunistic bacterial pathogens to adapt both to the host and the non-host
71 environment, (ii) manipulate the spatial structure of the environment, and (iii) uncover the targets
72 of selection and mechanisms provoking virulence change using high-throughput phenotypic
73 screening combined with whole-genome sequencing of evolved clones. For our approach, we
74 used the opportunistic human pathogen *Pseudomonas aeruginosa* infecting its model host, the
75 nematode *Caenorhabditis elegans* [31,32]. This bacterium is typically acquired by the host from
76 an environmental reservoir [33,34], and nematodes can quickly become infected through the
77 intestinal tract because they naturally feed on bacteria [35]. In our experiment, we let
78 *P. aeruginosa* PAO1 wildtype bacteria evolve for 60 days in four different environments in
79 eight-fold replication, implementing a 2x2 full factorial design (Fig. 1A). To assess the role of
80 spatial structure of the environment (first factor) for virulence evolution, we let the pathogens
81 evolve in either unstructured uniform liquid or spatially structured solid medium. To understand

82 how adaptation to the non-host environment affects virulence within the host, we further let the
83 pathogens evolve both in the presence and the absence of the host (second factor). Following
84 evolution, we quantified changes in pathogenicity for each independent replicate, and assessed
85 whether these changes are associated with alterations in the expression of four important
86 virulence factors of *P. aeruginosa*, which include the siderophore pyoverdine, the toxin
87 pyocyanin, secreted proteases, and the ability to form biofilms. Finally, we whole-genome
88 sequenced 140 evolved clones to map phenotypes to genotypes, and to test for positive selection,
89 parallel evolution among independent replicates, and orders of mutations during evolution.

90 MATERIALS AND METHODS

91 Strains and culturing conditions

92 *Pseudomonas aeruginosa* wildtype strain PAO1 (ATCC 15692) constitutively expressing GFP
93 (PAO1-*gfp*) was used for experimental evolution. The siderophore-deficient mutant
94 PAO1 Δ *pvdD-gfp*, the quorum-sensing deficient mutants PAO1 Δ *rhlR* and PAO1 Δ *lasR* (S.
95 Diggle, Georgia Institute of Technology, USA), and the biofilm-deficient mutant
96 MPAO1 Δ *pelA* Δ *pslA* (M. Toyofuku, University of Zurich, Switzerland) were used as negative
97 controls for phenotype screening. For overnight pre-culturing, we used Lysogeny Broth (LB) and
98 incubated cultures under shaking conditions (190 rpm) for 18-20 h. Optical density (OD) of
99 bacterial cultures was determined in a Tecan Infinite M-200 plate reader (Tecan Group Ltd.,
100 Switzerland) at a wavelength of 600 nm. All experiments were conducted at 25°C, except for
101 pre-culturing of the ancestral strain before experimental evolution (see below). To generate iron-
102 limited nutrient medium (RDM-Ch) suitable for bacterial and nematode co-culturing, we
103 supplied low-phosphate NGM (nematode growth medium; 2.5 gL⁻¹ BactoPeptone, 3 gL⁻¹ NaCl, 5
104 mgL⁻¹ Cholesterol, 25 mM MES buffer pH = 6.0, 1mM MgSO₄, 1mM CaCl₂; adapted from [32])
105 with 200 μ M of the iron chelator 2,2'-Bipyridyl. For agar plates, media were supplemented with
106 1.5% (m/V) agar. All chemicals were acquired from Sigma-Aldrich, Switzerland.
107 *Caenorhabditi elegans* N2 wildtype nematodes were acquired from the *Caenorhabditis Genetics*
108 *Center*. Nematode maintenance and generation of age-synchronized nematodes was performed
109 according to standard protocols [36].

110 **Experimental evolution**

111 Experimental evolution was started with a clonal population of PAO1-*gfp*. For each of the four
112 experimental treatments (agar plates with and without host, liquid culture with and without host),
113 eight replicate lines were evolved independently (Fig. 1). During experimental evolution,
114 *C. elegans* was not allowed to co-evolve. Instead, fresh L4-stage nematodes were supplied at
115 each transfer step. Since *P. aeruginosa* is highly virulent towards *C. elegans*, the vast majority of
116 worms were dead before each transfer step and we never observed any live larvae.

117
118 To start the experimental evolution, pre-cultures of PAO1-*gfp* were washed, OD-adjusted and
119 either spread onto RDM-Ch agar plates or inoculated into liquid RDM-Ch in culture tubes
120 (Fig. 1). For the “with host” treatments, L4-stage *C. elegans* nematodes were then added to each
121 plate/culture tube (details in Supplementary Material). Plates and culture tubes were incubated
122 for 48 h before the first transfer. Transfers of bacteria to fresh nutrient medium and, if applicable,
123 addition of fresh nematodes to the samples were conducted every 48 h (details in Supplementary
124 Material). Briefly: bacteria were transferred by replica-plating (for “agar plate” treatments) and a
125 fraction of nematodes was carried over (for “agar plates with host” treatments); or bacteria were
126 transferred by inoculating fresh media with an aliquot from the previous culture (for “liquid”
127 treatments), and a fraction of nematodes was carried over (for “liquid with host” treatments). The
128 number of viable bacteria transferred through replica-plating corresponded approximately to a
129 1:100 dilution, and was therefore equivalent to the dilution achieved in the liquid cultures. In
130 total, 30 transfers were conducted, corresponding to approximately 200 generations of bacterial
131 evolution. At the end of the experimental evolution, evolved populations were frozen at -80°C.

132

133 **Killing assays**

134 Population level virulence was assessed in two different killing assays at 25°C, namely in liquid
135 culture and on agar plates, representing the two different environments the bacterial populations
136 evolved in. Populations were separately tested both in the environment they evolved in
137 (populations evolved on agar plates tested on agar plates, and populations evolved in liquid
138 culture tested in liquid culture), and in the respective reciprocal environment (populations
139 evolved in liquid culture tested on agar plates, and vice versa).

140

141 For killing assays in liquid culture, evolved bacterial populations and the ancestral wildtype were
142 inoculated into liquid RDM-Ch in three replicate culture tubes per population. After an
143 incubation period of 48 h, ~2500 L4-stage nematodes were added, and culture tubes further
144 incubated for 48 h. Virulence was determined by counting the fraction of dead worms at 24 h and
145 48 h following nematode addition. For killing assays on agar plates, evolved bacterial
146 populations and the ancestral wildtype were spread on six replicate RDM-Ch agar plates per
147 population. Plates were then incubated for 48 h, and 20-60 L4-stage nematodes were added to
148 the plates. Virulence was determined by counting the fraction of dead worms at 24 h and 48 h
149 after adding the nematodes. More details on the killing assays can be found in the Supplementary
150 Material.

151

152 **Phenotypic screening of single clones**

153 Evolved bacterial populations were re-grown from freezer stocks and twenty colonies were
154 randomly isolated for each population. In total, 640 clones were isolated and subjected to
155 phenotypic screens for virulence factor production. Pyoverdine production was measured in

156 liquid RDM-Ch in 96-well plates. Plates were incubated for 24 h under shaken conditions and
157 OD600 and pyoverdine-specific fluorescence (ex: 400 nm / em: 460 nm) were measured in a
158 plate reader. Pyocyanin production was measured in liquid LB in 24-well plates. Plates were
159 incubated for 24 h under shaken conditions, and pyocyanin was quantified by measuring OD at
160 691 nm of the cell-free supernatant in a plate reader. Protease production was measured using
161 skim milk agar in 24-well plates. 1 μ L of bacterial culture was dropped onto the agar, and plates
162 were incubated for 20 h. Protease production was quantified by measuring the resulting halo with
163 ImageJ [37]. Biofilm production was measured in liquid LB in 96-well plates. Plates were
164 incubated under static conditions for 24 h, and the production of surface-attached biofilms was
165 quantified by calculating the “Biofilm Index” (OD570/OD550) for each well [38]. Details on the
166 phenotypic screening can be found in the Supplementary Material.

167

168 **Calculation of the “virulence factor index”**

169 We defined a virulence factor index $v = \sum r_i / n$, where r_i -values represent the average virulence
170 factor production scaled relative to the ancestral wildtype for the i -th virulence factor ($i =$
171 pyoverdine, pyocyanin, proteases, biofilm), and n is the total number of virulence factors. For
172 clones with wildtype production levels for all four virulence factors, $v = 1$, whereas $v < 1$ would
173 represent clones with overall reduced production levels. For statistical analyses and data
174 presentation, we used the average virulence index across clones for each population.

175

176 **Whole-genome sequencing of evolved clones**

177 To select populations and clones for sequencing, we first chose all populations with decreased
178 virulence, and then added randomly chosen populations to cover all four treatments in a balanced

179 way (four sequenced populations per treatment), leading to a total of 16 selected populations.
180 From these, we selected nine clones per population according to the following scheme: first, we
181 tried to get at least one clone that showed no phenotypic differences to the ancestral wildtype
182 with regards to pyoverdine and pyocyanin production. Then, we tried to get clones with a
183 marked decrease in pyoverdine and/or pyocyanin production. Finally, we filled up the list with
184 randomly chosen clones. Genomic DNA was isolated from all selected clones using a
185 commercial kit, sequencing libraries were constructed using the Nextera XT Kit (Illumina, USA)
186 and whole-genome sequencing was performed 2x150 bp on a NextSeq500 (Illumina, USA;
187 details in Supplementary Material).

188

189 **Variant calling**

190 Demultiplexed reads were aligned to the *P. aeruginosa* PAO1 reference genome using bowtie2
191 in local-sensitive mode [39]. PCR duplicates were removed using “picard” tools
192 (<https://broadinstitute.github.io/picard/>). Variants were called using “samtools” (v0.1.19),
193 “mpileup” and “bcftools” [40] and filtered with default parameters using “samtools” and
194 “vcfutils”. Variant effects were predicted using SnpEff (version 4.1d) [41]. Detailed protocols
195 for variant analysis and phylogenetic inference are provided in the Supplementary Material.

196

197 **Statistical Analysis**

198 We used linear models and linear mixed models for statistical analyses in R 3.2.2 [42]. When
199 data distributions did not meet the assumptions of linear models, we performed non-parametric
200 Wilcoxon rank-sum tests. To test whether virulence factor production in single clones depended
201 on the environment they evolved in, we used Markov-chain Monte Carlo generalized linear

202 mixed models (MCMCglmm) [43]. Principal component analysis (PCA) was conducted using
203 the ‘FactoMineR’ [44] and ‘factoextra’ packages ([https://CRAN.R-](https://CRAN.R-project.org/package=factoextra)
204 [project.org/package=factoextra](https://CRAN.R-project.org/package=factoextra)). Detailed description of statistical methods and test results are
205 provided in the Supplementary Methods and Table S1.

206 **RESULTS**

207 *Selection for reduced virulence in environments with low spatial structure*

208 Prior to experimental evolution, we found that the ancestral wildtype was highly virulent by
209 killing 76.2% and 83.9% of all host individuals within 24 hours in liquid and on solid media,
210 respectively (Table S2). This pattern changed during evolution in spatially unstructured
211 environments, where virulence dropped by 32.3% and 44.7% for populations that evolved with
212 and without hosts, respectively (Fig. 1B+C, Fig. S1). Conversely, virulence remained high in
213 structured environments. Overall, there was a significant effect of spatial structure on virulence
214 evolution (linear mixed model: $df_{\text{structure}} = 24.7$, $t_{\text{structure}} = -2.11$, $p_{\text{structure}} = 0.045$), while host
215 presence did not seem to matter ($df_{\text{host}} = 18.6$, $t_{\text{host}} = 0.86$, $p_{\text{host}} = 0.40$).

216

217 *Treatment-specific changes in virulence factor production*

218 To explore whether shareable virulence factors were under selection and whether changes in
219 virulence factor production could explain the evolution of virulence, we isolated 640 evolved
220 clones and quantified their production of: (i) pyoverdine, required for iron-scavenging [45]; (ii)
221 pyocyanin, a broad-spectrum toxin [46]; and (iii) proteases to digest extracellular proteins [47].
222 We further quantified the pathogens' ability to form biofilms on surfaces, another social trait
223 typically involved with virulence [48]. We focussed on these four virulence-related traits because
224 of their demonstrated relevance in the *C. elegans* infection model [32,48–50].

225

226 Our phenotype screens revealed significant treatment-specific changes in the production of all
227 four virulence factors (Fig. 2). For pyoverdine, we observed that production levels of evolved
228 clones were significantly lower in the unstructured environments without hosts compared to

229 the other treatments (Fig. 2A; Bayesian generalized linear mixed model, BGLMM, significant
230 interaction: $p_{\text{host:structure}} = 0.027$). Production levels were lower because many clones (44.4%)
231 have partially or completely lost the ability to produce pyoverdine (Fig. 2A). Since these
232 mutants appeared in six out of eight replicates (Fig. S2) and our media was iron-limited,
233 impeding the growth of pyoverdine non-producers, these clones likely represent social
234 cheaters, exploiting the pyoverdine secreted by producers [51,52]. While mutants with
235 abolished pyoverdine production also emerged in the unstructured environment with hosts,
236 their frequency was much lower (5.0%).

237
238 Pyocyanin production, meanwhile, significantly dropped in all four environments (Fig. 2B),
239 but more so in the presence than in the absence of the host ($p_{\text{host}} = 0.038$), while spatial
240 structure had no effect ($p_{\text{structure}} = 0.981$). The pattern of evolved protease production mirrored
241 the one for pyocyanin (Fig. 2C): there was a significant overall decrease in protease
242 production, with a significant host ($p_{\text{host}} = 0.042$), but no structure ($p_{\text{structure}} = 0.489$) effect.
243 Since neither pyocyanin nor proteases are necessary for growth in our media, consisting of a
244 protein-digest, reduced expression could reflect selection against dispensable traits. During
245 infections, however, these traits are known to be beneficial [49,50] and accelerated loss could
246 thus be explained by cheating, as secreted virulence factors could become exploitable inside
247 the host. It is known that protease production can be exploited by non-producing clones [47],
248 and there is recent evidence that the same might apply to pyocyanin [53]. The strong
249 correlation between the pyocyanin and protease phenotypic patterns is perhaps not surprising,
250 given that they are both regulated by the hierarchical quorum-sensing system of *P. aeruginosa*
251 [54].

252

253 Finally, the clones' ability to form surface-attached biofilms significantly increased in the
254 presence of the host ($p_{\text{host}} = 0.007$) and in structured environments ($p_{\text{structure}} = 0.010$; Fig. 2D).
255 These findings indicate that attachment ability might be less important under shaken conditions,
256 but relevant within the host to increase residence time.

257

258 *Aggregate change in virulence factor production correlates with evolved virulence*

259 While the phenotypic screens revealed altered virulence factor production levels, with significant
260 host and environmental effects (Fig. 2), the virulence data suggest that there is no host effect, and
261 spatial structure is the only determinant of virulence evolution (Fig 1). In the attempt to reconcile
262 these apparently conflicting results, we first performed a principal component analysis (PCA)
263 on population averages of the four virulence factor phenotypes (Fig. 3A). The PCA indicates
264 that each treatment evolved in a different direction in phenotype space, a pattern confirmed by a
265 PERMANOVA statistical analysis testing for spatial separation of treatment groups ($p = 0.002$).
266 From this, we can deduct that environmental and host factors indeed both seem to matter. This
267 analysis also shows that the direction of phenotypic changes was aligned for some traits, but
268 opposed for others (Fig. 3A, Fig. S3). A decrease in pyocyanin production was generally
269 connected to a decrease in protease production (Fig. S3D). On the other hand, decreased
270 pyocyanin and protease production were associated with both higher pyoverdine and biofilm
271 production (Fig. S3B+E).

272

273 Given these opposing evolutionary directions and trade-offs between virulence factors we
274 hypothesized that an increase in the production of one virulence factor could (at least partially)

275 be counterbalanced by the reduction of another virulence factor. In the extreme case, two
276 virulence factors could both be under selection, but in opposite directions, such that their net
277 effects on virulence could cancel out. In line with this hypothesis, we found that the evolutionary
278 change in virulence could only be explained when considering the aggregate change of all
279 virulence factor phenotypes (Fig. 3B, $R^2 = 0.33$, $F(1,30) = 14.7$, $p < 0.001$; also see Fig. S4),
280 but not when focussing on single virulence factors (Fig. S5). Thus, decreased virulence in
281 unstructured environments is attributable to a simultaneous decrease in the production of
282 multiple virulence factors (i.e. pyocyanin, proteases, and sometimes pyoverdine). Conversely,
283 unchanged virulence in structured environments can be explained by compensatory effects
284 (i.e. the reduction in pyocyanin and protease production is balanced by increased pyoverdine
285 and biofilm production). Important to note is that the observed pyoverdine upregulation is
286 presumably a compensatory phenotypic response, as decreased pyocyanin and protease
287 production are known to lower iron availability [55], which in turn might trigger increased
288 pyoverdine production.

289

290 *Mutations in key regulators explain changes in virulence factor phenotypes*

291 To examine whether genetic changes can explain the observed shifts in virulence factor
292 production, we successfully sequenced the genome of 140 evolved clones from 16 independent
293 populations and compared them to the ancestor. Relative to the ancestral wildtype, we identified
294 182 mutations (153 SNPs and 29 microindels, i.e. small insertions and deletions), with 5-49
295 mutations per population (median = 8.5). Individual clones accumulated 0-5 mutations, except
296 for one clone (PA-030) with 42 mutations, of which 41 mutations were in a 5022 bp Pfl
297 prophage region, a known mutational hotspot [56].

298
299 We identified 18 loci (genes and intergenic regions) that were independently mutated in at least
300 two populations (Fig. 4A). The most frequently mutated gene was *lasR*, encoding the regulator
301 of the Las quorum-sensing (QS) system. The second most frequent mutational target were ten
302 different *pil* genes, involved in type IV pili biosynthesis and twitching motility. The frequent
303 mutations in this cluster suggest that mutations in any of these genes could potentially lead to a
304 similar beneficial phenotype. Finally, the *pvdS* coding region or the *pvdG-pvdS* intergenic region,
305 containing the *pvdS* promoter, were also often mutated (i.e. in five populations). PvdS is the iron-
306 starvation sigma factor controlling pyoverdine synthesis, and mutations in this gene can lead to
307 pyoverdine deficiency [19,52].

308
309 We found that two of these frequently mutated targets explained a large proportion of the altered
310 virulence factor phenotypes (Fig. 5). Specifically, reduced pyoverdine production was
311 significantly associated with mutations in the *pvdS* gene or its promoter region ($F(1,137) =$
312 $240.1, p < 0.0001$, Fig. 5A). Moreover, there were significant correlations between reduced
313 pyocyanin and protease production and mutations in *lasR* (pyocyanin: $F(1,137) = 18.76, p <$
314 0.0001 ; proteases: $F(1,137) = 16.04, p < 0.001$, Fig. 5B+C). In roughly half of the clones
315 (pyocyanin: 51.3%, proteases: 45.6%), reduced production levels could be attributed to
316 mutations in *lasR*. While the Las-system directly controls the expression of proteases, pyocyanin
317 is only indirectly linked to this QS-system, via the two subordinate Rhl and PQS quorum sensing
318 systems [54]. We further analyzed whether the mutations in the type IV pili genes affected
319 biofilm formation. Although type IV pili can be important for bacterial attachment to surfaces
320 [57], there was no clear relationship between these mutations and the evolved biofilm

321 phenotypes (Fig. S6). This is probably because biofilm formation is a quantitative trait, involving
322 many genes, and because we found both evolution of increased and decreased biofilm
323 production, which complicates the phenotype-genotype matching. Alternatively, it could also be
324 that the observed mutations rather affect twitching motility than biofilm formation, a trait we did
325 not examine here, but might also be involved in virulence [58].

326

327 *Mutational patterns reveal evidence for positive selection and parallel evolution*

328 To test whether the mutated loci were under positive selection, we calculated the relative rates of
329 nonsynonymous to synonymous SNPs (dN/dS) for loci mutated in at least two populations and
330 for loci mutated only once. We found dN/dS = 6.2 for loci mutated in parallel in multiple
331 populations, suggesting significant positive selection ($P(X \geq 74) \sim \text{pois}(\lambda=12) < 0.0001$, where λ is
332 the expected number of nonsynonymous SNPs under neutral evolution and X is the observed
333 number of nonsynonymous SNPs). Conversely, dN/dS = 0.3 for loci mutated in only a single
334 population, indicating that these loci were under negative selection ($P(X \leq 26) \sim \text{pois}(\lambda=87) <$
335 0.0001). Altogether, our findings reveal that the 18 loci with multiple mutations underwent
336 adaptive parallel evolution.

337

338 Finally, we used phylogenetic inference to resolve the order of mutations involving the *lasR*,
339 *pvdS*, and *pil* genes (Fig. 4B, Table S3). Such analyses could reveal whether selection of
340 mutations in certain genes is dependent on previous mutations in other genes. When analyzing
341 evolved clones that mutated in at least two of these loci, we observed no clear patterns of
342 dependencies in the order of mutations in *lasR-pil*-mutants and *lasR-pvdS*-mutants. For *pvdS-pil*-
343 mutants, meanwhile, we found that mutations in *pvdS* tended to precede the mutations in *pil*

344 genes. While sample size is too low to draw any strong conclusions, this observation could
345 indicate that mutations in type IV pili are particularly beneficial in a pyoverdine-negative
346 background.

347 **DISCUSSION**

348 Using the opportunistic human pathogen *P. aeruginosa*, we show that bacterial virulence can
349 evolve rapidly during experimental evolution, as a result of adaptation to both the host and the
350 non-host environment. Overall, we found that *P. aeruginosa* evolved greatly reduced virulence
351 in liquid unstructured environments, but remained highly virulent in spatially structured
352 environments, regardless of whether its nematode host was present or absent. Phenotypic and
353 genotypic screens provide strong evidence for positive selection on bacterial virulence factors
354 and parallel adaptive evolution across independent replicates. Virulence reduction in
355 unstructured environments without hosts was driven by a sharp decline in the production of the
356 siderophore pyoverdine, and moderate decreases in protease and pyocyanin production.
357 Conversely, virulence reduction in unstructured environment with hosts is explained by a stark
358 decrease in protease and pyocyanin production, but not pyoverdine. Although the traits under
359 selection seem to vary as a function of host presence, our findings are in strong support of
360 evolutionary theory predicting that low spatial structure should select for reduced pathogenicity
361 if virulence is mediated by secreted compounds such as toxins, proteases or siderophores [5,9].
362 The reason for this is that secreted virulence factors can be shared between cells, and can thus
363 become exploitable by cheating mutants that no longer contribute to costly virulence factor
364 production, yet still capitalize on those produced by others. The spread of such mutants is
365 predicted to reduce overall virulence factor availability and to curb virulence, exactly as
366 observed in our study.

367

368 Our results highlight how an in-depth mechanistic analysis of the traits under selection can
369 deepen our understanding of virulence evolution. In the absence of our phenotypic and genetic

370 trait analysis, we would be tempted to conclude that the presence of the host has no effect on
371 virulence evolution, and that evolutionary change is entirely driven by the external non-host
372 environment (Fig. 2). Our mechanistic trait analysis shows that such conclusions would be
373 premature and yields several novel nuances of virulence evolution. First, we observed strong
374 selection for pyoverdine-negative mutants only in the absence but not in the presence of the host
375 (Fig. 2A). Pervasive selection against pyoverdine in unstructured, yet iron-limited medium, has
376 previously been attributed to cheating [14]. Here, we show that the spread of pyoverdine non-
377 producers is apparently prevented in the presence of the host. One reason for this host-specific
378 effect might be that the spatial structure inside hosts counteracts the selective advantage non-
379 producers experience outside the host. Second, we found that the presence of the host had a
380 significant effect on the strength of selection against pyocyanin and protease production (Fig.
381 2B+C). We speculate that the presence of the host alters the reason for why these two virulence
382 factors are selected against. In the absence of the host, neither pyocyanin nor proteases are
383 required for growth, and their decline could be explained by selection against superfluous traits.
384 Conversely, these two traits become beneficial in the presence of the host [49,50], such that
385 selection against them could at least partially be explained by cheating. Third, we found evidence
386 that the presence of the host selected for mutants with increased capacities to form biofilms (Fig.
387 2D). Apart from increasing residency time within hosts, the shift from a planktonic to a more
388 sessile lifestyle typically goes along with fundamental changes in gene expression patterns
389 [59,60], which might in turn affect virulence. Finally, we found that virulence factors were also
390 under selection in treatments where the overall virulence level did not change (i.e. in structured
391 environments). In these environments, however, reduced production of one virulence factor (e.g.
392 protease and pyocyanin) was often compensated by the upregulation of other virulence factors

393 (e.g. pyoverdine and biofilm), resulting in a zero net change in virulence.

394

395 A number of previous studies showed that when competition between virulence-factor producing
396 and engineered non-producing bacteria is allowed for, then non-producing strains can often
397 invade pathogen populations and thereby lower virulence [15,17,23,24]. While our work is in
398 line with these findings, it makes several additional contributions. First, our experiment started
399 with fully virulent clonal wildtype bacteria, and any virulence-factor deficient mutants had to
400 evolve from random mutations and invade pathogen populations from extreme rarity. Hence, our
401 study proves that the predicted mutants indeed arise *de novo* and are promoted by natural
402 selection in independent parallel replicates. Second, our results highlight that multiple social
403 traits are under selection simultaneously, which can lead to either additive effects (when traits
404 are regulatorily linked, e.g. proteases and pyocyanin) or compensatory effects (when traits
405 evolve in opposite directions, e.g. increased biofilm versus decreased protease production).
406 Third, our study design captured the cycling of an opportunistic pathogen through the host and
407 the non-host environment, as it would occur under natural conditions [26,27], an approach that
408 allowed us to discover accidental virulence effects that are purely driven by adaptation to the
409 non-host environment.

410

411 At the genetic level, our findings closely relate to previous work that has identified *lasR* as a key
412 target of evolution in the context of chronic *P. aeruginosa* infections in the cystic fibrosis lung
413 [61–65], in non-cystic fibrosis bronchiectasis [66], as well as in acute infections [18,29]. While
414 the ubiquitous appearance of *lasR*-mutants was often interpreted as a specific host adaptation, we
415 show here that *lasR*-mutants frequently arise even in the absence of a host, indicating that

416 mutations in *lasR* are not a host-specific phenomenon. We propose three mutually non-exclusive
417 explanations for the frequent occurrence and selective spread of *lasR*-mutants. First, we propose
418 that the Las-quorum-sensing regulon might no longer be beneficial under many of the culturing
419 conditions used in the laboratory, especially when bacteria are consistently grown at high cell
420 densities. Mutations in *lasR* would thus reflect the first step in the degradation of this system.
421 Alternatively, it is conceivable that quorum sensing remains beneficial, but that mutations in
422 *lasR* represent the first step in the rewiring of the QS network in order to customize it to the
423 novel conditions experienced in infections and laboratory cultures [67]. Finally, the invasion of
424 *lasR*-mutants could be the result of cheating, where these signal blind mutants still contribute to
425 signal production, but no longer respond to it and thus refrain from producing the QS-controlled
426 public goods [47,68]. We have argued above that, although *lasR* mutants were favoured in all our
427 treatments, the presence of the host might change the selection pressure and underlying reason
428 for why these mutants are selected for. More generally, our observations of high strain
429 diversification during experimental evolution, and the co-existence of multiple different
430 phenotypes and genotypes within each replicate, are reminiscent of patterns found in chronic *P.*
431 *aeruginosa* infections in cystic fibrosis lungs [19,61,62,69–72]. While this diversity might be
432 transient in some cases, it highlights that an initially clonal infection can give rise to a diverse
433 community, with multiple strains competing with each other within the host, as it was observed
434 in CF lung communities [73,74]. Despite these striking similarities, we need to be careful when
435 extrapolating from a nematode gut to a human lung environment. Clearly, more studies in other
436 host organisms are required to identify common evolutionary patterns in infections. Moreover,
437 analysis of intermediate time points and additional virulence factors could further deepen our
438 understanding of temporal evolutionary patterns and virulence traits under selection.

439

440 In conclusion, our study demonstrates that there is rapid and parallel virulence evolution in
441 populations of the opportunist *P. aeruginosa*, and that secreted virulence factors are the main
442 target of selection. While low spatial structure of the environment generally selected for lower
443 virulence regardless of whether hosts were present or not, the virulence traits under selection and
444 the strength of selection were host dependent. This greatly contributes to our knowledge on how
445 bacterial opportunistic pathogens adapt to the variable environments they occupy, and how this
446 affects their virulence [26,27]. Our work also highlights that linking virulence evolution to
447 selection inside and outside of the host is key to predict evolutionary trajectories in opportunistic
448 pathogens. Such insights might offer simple approaches of how to manage infections in these
449 clinically highly important pathogens [69,75–77], for example through the disruption of spatial
450 structure in chronic infections, which could, according to our findings, steer pathogen evolution
451 towards lower virulence.

452

453 **DATA AVAILABILITY**

454 All sequencing data generated for this study are available from the European Nucleotide Archive
455 (accession number PRJEB23190). All other raw datasets have been deposited in the Figshare
456 repository (doi:).

457

458 **SUPPLEMENTARY INFORMATION**

459 Supplementary information is available at ISME's website.

460

461 **ACKNOWLEDGEMENTS**

462 We thank Swati Parekh for assistance in genomic analysis, Isa Moreno for help with the

463 nematode killing assays, Ruben Dezeure for statistical advice, and Stu West and Sam Brown for
464 comments on the manuscript.

465

466 **COMPETING INTERESTS**

467 The authors declare no competing financial interests.

468 **REFERENCES**

- 469 1. Cressler CE, McLeod D V., Rozins C, Van den Hoogen J, Day T. The adaptive evolution
470 of virulence: a review of theoretical predictions and empirical tests. *Parasitology*.
471 2016;143(07):915–30.
- 472 2. Diard M, Hardt W-D. Evolution of bacterial virulence. *FEMS Microbiol Rev*.
473 2017;41:679–97.
- 474 3. Frank SA. Models of Parasite Virulence. *Q Rev Biol*. 1996;71(1):37–78.
- 475 4. Wild G, Gardner A, West SA. Adaptation and the evolution of parasite virulence in a
476 connected world. *Nature*. 2009;459(7249):983–6.
- 477 5. Buckling A, Brockhurst MA. Kin selection and the evolution of virulence. *Heredity*.
478 2008;100(5):484–8.
- 479 6. Lion S. Multiple infections, kin selection and the evolutionary epidemiology of parasite
480 traits. *J Evol Biol*. 2013;26(10):2107–22.
- 481 7. Alizon S, de Roode JC, Michalakis Y. Multiple infections and the evolution of virulence.
482 *Ecol Lett*. 2013;16(4):556–67.
- 483 8. de Roode JC, Pansini R, Cheesman SJ, Helinski MEH, Huijben S, Wargo AR, et al.
484 Virulence and competitive ability in genetically diverse malaria infections. *Proc Natl Acad
485 Sci U S A*. 2005;102(21):7624–8.
- 486 9. West SA, Buckling A. Cooperation, virulence and siderophore production in bacterial
487 parasites. *Proc Biol Sci*. 2003;270(1510):37–44.
- 488 10. Alizon S, Lion S. Within-host parasite cooperation and the evolution of virulence. *Proc
489 Biol Sci*. 2011;278(1725):3738–47.
- 490 11. West SA, Diggle SP, Buckling A, Gardner A, Griffin AS. The Social Lives of Microbes.
491 *Annu Rev Ecol Evol Syst*. 2007;38(1):53–77.
- 492 12. Brown SP, Hochberg ME, Grenfell BT. Does multiple infection select for raised
493 virulence? *Trends Microbiol*. 2002;10(9):401–5.
- 494 13. Buckling A, Harrison F, Vos M, Brockhurst MA, Gardner A, West SA, et al. Siderophore-
495 mediated cooperation and virulence in *Pseudomonas aeruginosa*. *FEMS Microbiol Ecol*.
496 2007;62(2):135–41.
- 497 14. Kümmerli R, Griffin AS, West SA, Buckling A, Harrison F. Viscous medium promotes
498 cooperation in the pathogenic bacterium *Pseudomonas aeruginosa*. *Proc Biol Sci*.

- 499 2009;276(1672):3531–8.
- 500 15. Harrison F, Browning LE, Vos M, Buckling A. Cooperation and virulence in acute
501 *Pseudomonas aeruginosa* infections. *BMC Biol.* 2006;4:21.
- 502 16. Raymond B, West SA, Griffin AS, Bonsall MB. The dynamics of cooperative bacterial
503 virulence in the field. *Science.* 2012;337(6090):85–8.
- 504 17. Rumbaugh KP, Diggle SP, Watters CM, Ross-Gillespie A, Griffin AS, West SA. Quorum
505 Sensing and the Social Evolution of Bacterial Virulence. *Curr Biol.* 2009;19(4):341–5.
- 506 18. Köhler T, Buckling A, van Delden C. Cooperation and virulence of clinical *Pseudomonas*
507 *aeruginosa* populations. *Proc Natl Acad Sci U S A.* 2009;106(15):6339–44.
- 508 19. Andersen SB, Marvig RL, Molin S, Krogh Johansen H, Griffin AS. Long-term social
509 dynamics drive loss of function in pathogenic bacteria. *Proc Natl Acad Sci.*
510 2015;112(34):10756–61.
- 511 20. Boots M, Meador M. Local interactions select for lower pathogen infectivity. *Science.*
512 2007;315(5816):1284–6.
- 513 21. Kerr B, Neuhauser C, Bohannan BJM, Dean AM. Local migration promotes competitive
514 restraint in a host-pathogen “tragedy of the commons”. *Nature.* 2006;442(7098):75–8.
- 515 22. Leggett HC, Wild G, West SA, Buckling A, Leggett HC. Fast-killing parasites can be
516 favoured in spatially structured populations. *Philos Trans R Soc Lond B Biol Sci.*
517 2017;372(1719):1–5.
- 518 23. Rumbaugh KP, Trivedi U, Watters C, Burton-Chellew MN, Diggle SP, West SA. Kin
519 selection, quorum sensing and virulence in pathogenic bacteria. *Proc R Soc B Biol Sci.*
520 2012;279(1742):3584–8.
- 521 24. Pollitt EJG, West SA, Crusz S a, Burton-Chellew MN, Diggle SP. Cooperation, Quorum
522 Sensing, and Evolution of Virulence in *Staphylococcus aureus*. *Infect Immun.*
523 2014;82(3):1045–51.
- 524 25. Leggett HC, Cornwallis CK, Buckling A, West SA. Growth rate, transmission mode and
525 virulence in human pathogens. *Philos Trans R Soc B Biol Sci.* 2017;372(1719):20160094.
- 526 26. Brown SP, Cornforth DM, Mideo N. Evolution of virulence in opportunistic pathogens:
527 generalism, plasticity, and control. *Trends Microbiol.* 2012;20(7):336–42.
- 528 27. Brown NF, Wickham ME, Coombes BK, Finlay BB. Crossing the line: Selection and
529 evolution of virulence traits. *PLoS Pathog.* 2006;2(5):346–53.

- 530 28. Racey D, Inglis RF, Harrison F, Oliver A, Buckling A. The effect of elevated mutation
531 rates on the evolution of cooperation and virulence of *Pseudomonas aeruginosa*.
532 *Evolution*. 2010;64(2):515–21.
- 533 29. Jansen G, Crummenerl LL, Gilbert F, Mohr T, Pfefferkorn R, Thänert R, et al.
534 Evolutionary transition from pathogenicity to commensalism: Global regulator mutations
535 mediate fitness gains through virulence attenuation. *Mol Biol Evol*. 2015;32(11):2883–96.
- 536 30. Ford SA, Kao D, Williams D, King KC. Microbe-mediated host defence drives the
537 evolution of reduced pathogen virulence. *Nat Commun*. 2016;7.
- 538 31. Tan MW, Mahajan-Miklos S, Ausubel FM. Killing of *Caenorhabditis elegans* by
539 *Pseudomonas aeruginosa* used to model mammalian bacterial pathogenesis. *Proc Natl*
540 *Acad Sci U S A*. 1999;96(2):715–20.
- 541 32. Zaborin A, Romanowski K, Gerdes S, Holbrook C, Lepine F, Long J, et al. Red death in
542 *Caenorhabditis elegans* caused by *Pseudomonas aeruginosa* PAO1. *Proc Natl Acad Sci U*
543 *S A*. 2009;106(15):6327–32.
- 544 33. de Abreu P, Farias P, Paiva G, Almeida A, Morais P. Persistence of microbial
545 communities including *Pseudomonas aeruginosa* in a hospital environment: a potential
546 health hazard. *BMC Microbiol*. 2014;14(1):118.
- 547 34. Green S, Schroth M, Cho J. Agricultural plants and soil as a reservoir for *Pseudomonas*
548 *aeruginosa*. *Appl Microbiol*. 1974;28(6):987–91.
- 549 35. Samuel BS, Rowedder H, Braendle C, Félix M-A, Ruvkun G. *Caenorhabditis elegans*
550 responses to bacteria from its natural habitats. *Proc Natl Acad Sci*. 2016;113(27):E3941–
551 9.
- 552 36. Stiernagle T. Maintenance of *C. elegans*. *WormBook*: the online review of *C. elegans*
553 biology. *WormBook*; 2006. 1-11 p.
- 554 37. Rasband WS. *ImageJ*. Bethesda, Maryland, USA: U. S. National Institutes of Health;
555 1997.
- 556 38. Savoia D, Zucca M. Clinical and environmental *Burkholderia* Strains: Biofilm production
557 and intracellular survival. *Curr Microbiol*. 2007;54(6):440–4.
- 558 39. Langmead B, Salzberg SL. Fast gapped-read alignment with Bowtie 2. *Nat Methods*.
559 2012;9(4):357–60.
- 560 40. Li H. A statistical framework for SNP calling, mutation discovery, association mapping

- 561 and population genetical parameter estimation from sequencing data. *Bioinformatics*.
562 2011;27(21):2987–93.
- 563 41. Cingolani P, Platts A, Wang LL, Coon M, Nguyen T, Wang L, et al. A program for
564 annotating and predicting the effects of single nucleotide polymorphisms, SnpEff: SNPs in
565 the genome of *Drosophila melanogaster* strain w 1118; iso-2; iso-3. *Fly*. 2012;6(2):80–92.
- 566 42. R Development Core Team. R: A language and environment for statistical computing.
567 Vienna, Austria: R Foundation for Statistical Computing; 2016.
- 568 43. Hadfield JD. MCMC methods for multi-response generalized linear mixed models: The
569 MCMCglmm R package. *J Stat Softw*. 2010;33(2):1–22.
- 570 44. Le S, Josse J, Husson F. FactoMineR: An R Package for Multivariate Analysis. *J Stat*
571 *Softw*. 2008;25(1):1–18.
- 572 45. Schalk IJ, Guillon L. Pyoverdine biosynthesis and secretion in *Pseudomonas aeruginosa*:
573 implications for metal homeostasis. *Environ Microbiol*. 2013;15(6):1661–73.
- 574 46. Lau GW, Hasset DJ, Ran H, Kong F. The role of pyocyanin in *Pseudomonas aeruginosa*
575 infection. *Trends Mol Med*. 2004;10(12):599–606.
- 576 47. Diggle SP, Griffin AS, Campbell GS, West SA. Cooperation and conflict in quorum-
577 sensing bacterial populations. *Nature*. 2007;450(7168):411–4.
- 578 48. van Tilburg Bernardes E, Charron-Mazenod L, Reading DJ, Reckseidler-Zenteno SL,
579 Lewenza S. Exopolysaccharide-repressing small molecules with antibiofilm and
580 antivirulence activity against *Pseudomonas aeruginosa*. *Antimicrob Agents Chemother*.
581 2017;61(5):AAC.01997-16.
- 582 49. Cezairliyan B, Vinayavekhin N, Grenfell-Lee D, Yuen GJ, Saghatelian A, Ausubel FM.
583 Identification of *Pseudomonas aeruginosa* phenazines that kill *Caenorhabditis elegans*.
584 *PLoS Pathog*. 2013;9(1).
- 585 50. Zhu J, Cai X, Harris TL, Gooyit M, Wood M, Lardy M, et al. Disarming *Pseudomonas*
586 *aeruginosa* Virulence Factor LasB by Leveraging a *Caenorhabditis elegans* Infection
587 Model. *Chem Biol*. 2015;22(4):483–91.
- 588 51. Dumas Z, Kümmerli R. Cost of cooperation rules selection for cheats in bacterial
589 metapopulations. *J Evol Biol*. 2012;25(3):473–84.
- 590 52. Kümmerli R, Santorelli LA, Granato ET, Dumas Z, Dobay A, Griffin AS, et al. Co-
591 evolutionary dynamics between public good producers and cheats in the bacterium

- 592 *Pseudomonas aeruginosa*. *J Evol Biol*. 2015;28(12):2264–74.
- 593 53. Ross-Gillespie A, Weigert M, Brown SP, Kümmerli R. Gallium-mediated siderophore
594 quenching as an evolutionarily robust antibacterial treatment. *Evol Med Public Heal*.
595 2014;2014(1):18–29.
- 596 54. Lee J, Zhang L. The hierarchy quorum sensing network in *Pseudomonas aeruginosa*.
597 *Protein Cell*. 2014;6(1):26–41.
- 598 55. Bonchi C, Frangipani E, Imperi F, Visca P. Pyoverdine and proteases affect the response
599 of *pseudomonas aeruginosa* to gallium in human serum. *Antimicrob Agents Chemother*.
600 2015;59(9):5641–6.
- 601 56. Lim WS, Phang KKS, Tan AHM, Li SFY, Ow DSW. Small colony variants and single
602 nucleotide variations in Pfl region of Pb1 phage-resistant *Pseudomonas aeruginosa*. *Front*
603 *Microbiol*. 2016;7:1–14.
- 604 57. Barken KB, Pamp SJ, Yang L, Gjermansen M, Bertrand JJ, Klausen M, et al. Roles of
605 type IV pili, flagellum-mediated motility and extracellular DNA in the formation of
606 mature multicellular structures in *Pseudomonas aeruginosa* biofilms. *Environ Microbiol*.
607 2008;10(9):2331–43.
- 608 58. Marko VA, Kilmury SLN, MacNeil LT, Burrows LL. *Pseudomonas aeruginosa* type IV
609 minor pilins and PilY1 regulate virulence by modulating FimS-AlgR activity. Lee VT,
610 editor. *PLoS Pathog*. 2018;14(5):e1007074.
- 611 59. Sauer K, Camper AK, Ehrlich GD, Costerton JW, Davies DG. *Pseudomonas aeruginosa*. *J*
612 *Bacteriol*. 2002;184(4):1140–54.
- 613 60. Rollet C, Gal L, Guzzo J. Biofilm-detached cells, a transition from a sessile to a
614 planktonic phenotype: A comparative study of adhesion and physiological characteristics
615 in *pseudomonas aeruginosa*. *FEMS Microbiol Lett*. 2009;290(2):135–42.
- 616 61. Marvig RL, Sommer LM, Molin S, Johansen HK. Convergent evolution and adaptation of
617 *Pseudomonas aeruginosa* within patients with cystic fibrosis. *Nat Genet*. 2015;47(1):57–
618 65.
- 619 62. Winstanley C, O’Brien S, Brockhurst MA. *Pseudomonas aeruginosa* Evolutionary
620 Adaptation and Diversification in Cystic Fibrosis Chronic Lung Infections. *Trends*
621 *Microbiol*. 2016;24(5):327–37.
- 622 63. Hoffman LR, Kulasekara HD, Emerson J, Houston LS, Burns JL, Ramsey BW, et al.

- 623 Pseudomonas aeruginosa lasR mutants are associated with cystic fibrosis lung disease
624 progression. *J Cyst Fibros.* 2009;8(1):66–70.
- 625 64. Yang L, Jelsbak L, Marvig RL, Damkiær S, Workman CT, Rau MH, et al. Evolutionary
626 dynamics of bacteria in a human host environment. *Proc Natl Acad Sci.*
627 2011;108(18):7481–6.
- 628 65. Smith EE, Buckley DG, Wu Z, Saenphimmachak C, Hoffman LR, D’Argenio DA, et al.
629 Genetic adaptation by *Pseudomonas aeruginosa* to the airways of cystic fibrosis patients.
630 *Proc Natl Acad Sci U S A.* 2006;103(22):8487–92.
- 631 66. Woo TE, Duong J, Jervis NM, Rabin HR, Parkins MD, Storey DG, et al. Virulence
632 adaptations of *Pseudomonas aeruginosa* isolated from patients with non-cystic fibrosis
633 bronchiectasis. *Microbiology.* 2016;162(12):2126–35.
- 634 67. Feltner JB, Wolter DJ, Pope CE, Groleau MC, Smalley NE, Greenberg EP, et al. LasR
635 variant cystic fibrosis isolates reveal an adaptable quorum-sensing hierarchy in
636 *Pseudomonas aeruginosa*. *MBio.* 2016;7(5):1–9.
- 637 68. Sandoz KM, Mitzimberg SM, Schuster M. Social cheating in *Pseudomonas aeruginosa*
638 quorum sensing. *Proc Natl Acad Sci.* 2007;104(40):15876–81.
- 639 69. Folkesson A, Jelsbak L, Yang L, Johansen HK, Ciofu O, Høiby N, et al. Adaptation of
640 *Pseudomonas aeruginosa* to the cystic fibrosis airway: an evolutionary perspective. *Nat*
641 *Rev Microbiol.* 2012;10(12):841–51.
- 642 70. Jorth P, Staudinger BJ, Wu X, Hisert KB, Hayden H, Garudathri J, et al. Regional
643 Isolation Drives Bacterial Diversification within Cystic Fibrosis Lungs. *Cell Host*
644 *Microbe.* 2015;18(3):307–19.
- 645 71. Williams D, Evans B, Haldenby S, Walshaw MJ, Brockhurst MA, Winstanley C, et al.
646 Divergent, coexisting *Pseudomonas aeruginosa* lineages in chronic cystic fibrosis lung
647 infections. *Am J Respir Crit Care Med.* 2015;191(7):775–85.
- 648 72. Williams D, Fothergill JL, Evans B, Caples J, Haldenby S, Walshaw MJ, et al.
649 Transmission and lineage displacement drive rapid population genomic flux in cystic
650 fibrosis airway infections of a *Pseudomonas aeruginosa* epidemic strain. *Microb*
651 *Genomics.* 2018;4(3).
- 652 73. O’Brien S, Williams D, Fothergill JL, Paterson S, Winstanley C, Brockhurst MA. High
653 virulence sub-populations in *Pseudomonas aeruginosa* long-term cystic fibrosis airway

- 654 infections. *BMC Microbiol.* 2017;17(1):30.
- 655 74. Mowat E, Paterson S, Fothergill JL, Wright EA, Ledson MJ, Walshaw MJ, et al.
656 *Pseudomonas aeruginosa* population diversity and turnover in cystic fibrosis chronic
657 infections. *Am J Respir Crit Care Med.* 2011;183(12):1674–9.
- 658 75. Peleg AY, Hooper DC. Hospital Acquired Infections Due to Gram-Negative Bacteria. *N*
659 *Engl J Med.* 2011;362(19):1804–13.
- 660 76. Gaynes R, Edwards JR. Overview of nosocomial infections caused by gram-negative
661 bacilli. *Clin Infect Dis.* 2005;41(6):848–54.
- 662 77. Cosgrove SE, Carmeli Y. The Impact of Antimicrobial Resistance on Health and
663 Economic Outcomes. *Clin Infect Dis.* 2003;36:1433–7.
- 664

665 **FIGURE LEGENDS**

666 **Fig. 1. Virulence decreased during evolution in spatially unstructured environments. (A)**

667 Experimental design: *P. aeruginosa* PAO1 bacteria were serially transferred 30 times in four
668 different environments in 8-fold replication. These environments were either spatially structured
669 (“struc +”) or unstructured (“struc –“), and either contained (“host +”) or did not contain
670 (“host –“) *C. elegans* nematodes for the bacteria to infect. Subsequently, the evolved populations
671 were tested for their virulence towards the nematode under two different conditions: **(B)** In the
672 environment the populations evolved in (i.e. populations that evolved on agar plates tested on
673 agar plates, populations that evolved in liquid culture tested in liquid culture); and **(C)** in the
674 reciprocal environment as a control (populations that evolved on agar plates tested in liquid
675 culture, populations that evolved in liquid tested on agar plates). Both assays revealed that
676 virulence significantly decreased during evolution in unstructured environments (Wilcoxon rank-
677 sum test, asterisks denote $p < 0.05$; see Table S1). Virulence was quantified as percent
678 nematodes killed at 24 h post infection, scaled to the ancestral wildtype. Individual dots represent
679 mean virulence of evolved populations across three replicates. The red line represents the
680 average wildtype virulence level in the respective assay, with shaded areas denoting the 95%
681 confidence intervals.

682

683 **Fig. 2. Selection promoted shifts in virulence factor production during experimental**

684 **evolution.** The production levels of four important virulence factors were determined for 640
685 evolved *P. aeruginosa* clones (20 clones per evolved line), and compared to the ancestral
686 wildtype (mean \pm 95 % confidence intervals indicated as red lines and shaded areas,
687 respectively). **(A)** Pyoverdine production significantly increased in all treatments, except in the

688 host-free unstructured environment, where 44% of all evolved clones partially or completely lost
689 the ability to produce this siderophore. **(B)** The production of the toxin pyocyanin significantly
690 decreased in all environments, but more so in the environments with the host. **(C)** The
691 production of proteases also significantly decreased in all environments, with a sharper decline in
692 environments with the host. **(D)** The clones' ability to form surface-attached biofilms
693 significantly decreased in the unstructured host-free environment, but significantly increased in
694 all other environments. host (−) = host was absent during evolution; host (+) = host was present
695 during evolution; struc (−) = evolution in a liquid-shaken unstructured environment; struc (+) =
696 evolution in a structured environment on agar. We used non-parametric Wilcoxon rank-sum test
697 for comparisons relative to the ancestral wildtype (asterisks denote $p < 0.05$), and BGLMM to
698 test for treatment effects (see Table S1). Solid black bars denote the median for each treatment.

699

700 **Fig. 3. The aggregate change in virulence factor production explains virulence evolution.**

701 **(A)** A principal component analysis (PCA) on the population-level changes in the production of
702 four virulence factors (pyoverdine, pyocyanin, proteases, biofilm) reveals divergent evolutionary
703 patterns. For instance, analysis of the first two principal components (explaining 80.6 % of the
704 total variance) shows complete segregation between populations evolved in unstructured host-
705 free environments and structured environments with the host. Moreover, the PCA reveals that
706 evolutionary change was aligned for some traits (aligned vectors for pyocyanin and proteases),
707 but opposed for others (inversed vectors for pyoverdine versus pyocyanin/proteases). Small and
708 large symbols depict individual population values and average values per environment,
709 respectively. Polygons show the boundaries in phenotype space for each environment. **(B)** We
710 found that the aggregate change in the production of all four virulence factors explained the

711 evolution of virulence. To account for the aligned and opposing effects revealed by the PCA, we
712 defined the “virulence factor index” as the average change in virulence factor production across
713 all four traits, scaled relative to the ancestral wildtype. Symbols and error bars depict mean
714 values per population and standard errors of the mean, respectively.

715

716 **Fig. 4. Whole genome sequencing reveals mutational profiles and order of mutations.**

717 Whole genomes of 140 evolved clones (four populations per environment and eight to nine
718 clones per population) were sequenced, and SNPs and INDELs in genes and intergenic regions
719 were called relative to the ancestral wildtype. **(A)** List of the loci that harbored mutations in at
720 least two populations. The scale of grey shadings corresponds to the number of populations from
721 each experimental condition in which clones with mutations in the respective loci occurred. **(B)**
722 Phylogenetic interference of the order of mutations among clones harboring mutations in two of
723 the most frequently affected loci. Order of mutations are indicated by arrows pointing towards
724 the loci that were mutated second. Lines without arrowheads indicate that phylogenetic inference
725 could not resolve the order of mutations.

726

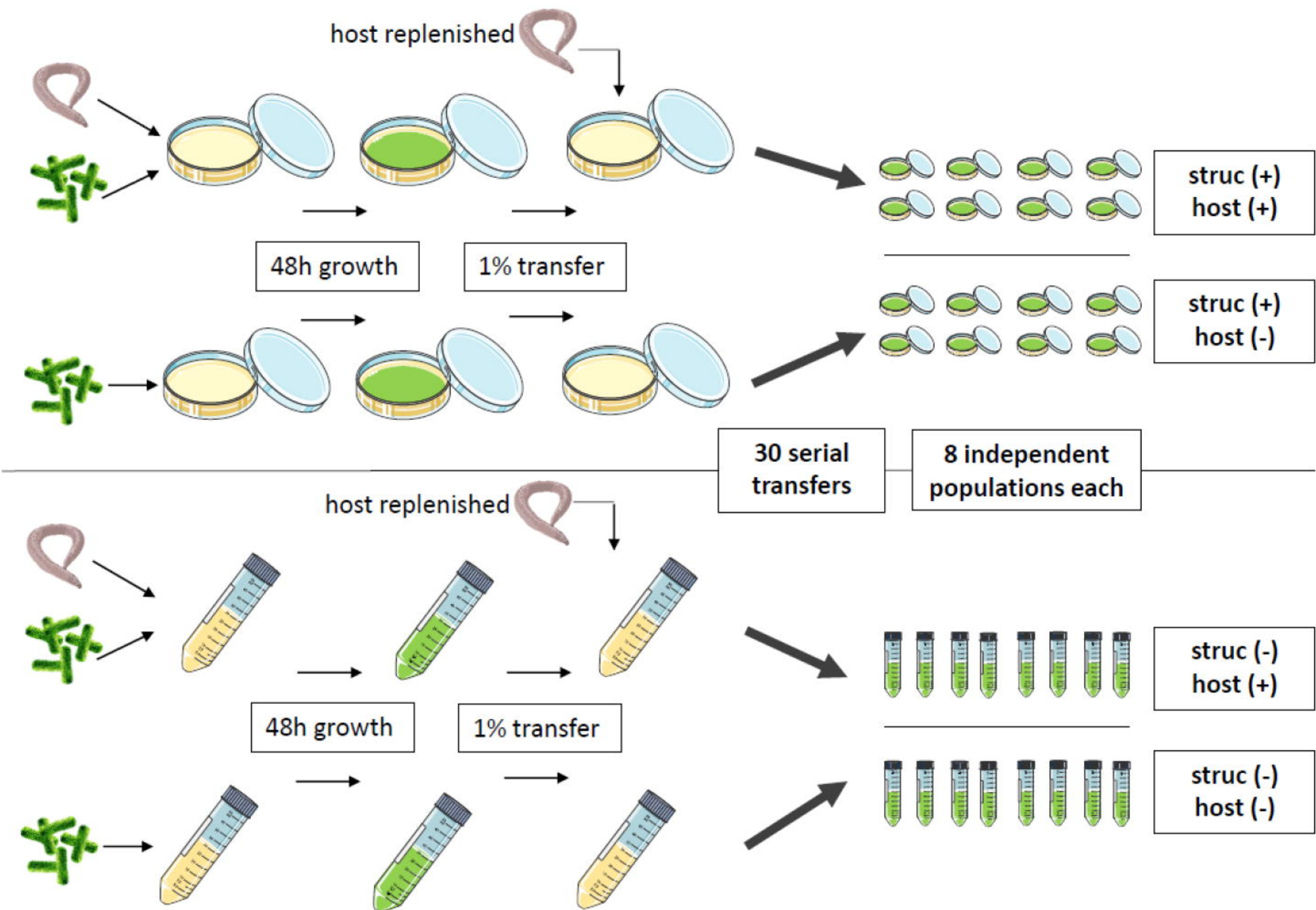
727 **Fig. 5. Mutations in key regulatory genes underlie the loss of virulence factor production.**

728 Across the 140 sequenced clones, there was an accumulation of mutations in two regulatory
729 genes (*pvdS* and *lasR*), which significantly correlated with the phenotypic changes observed for
730 pyoverdine **(A)**, pyocyanin **(B)** and protease **(C)** production. *pvdS* encodes the iron starvation
731 sigma factor and all clones with mutations in this gene or its promoter showed significantly
732 impaired pyoverdine production. *lasR* encodes the regulator of the Las-quorum-sensing system,
733 which directly controls the expression of several proteases. All clones with *lasR* mutations

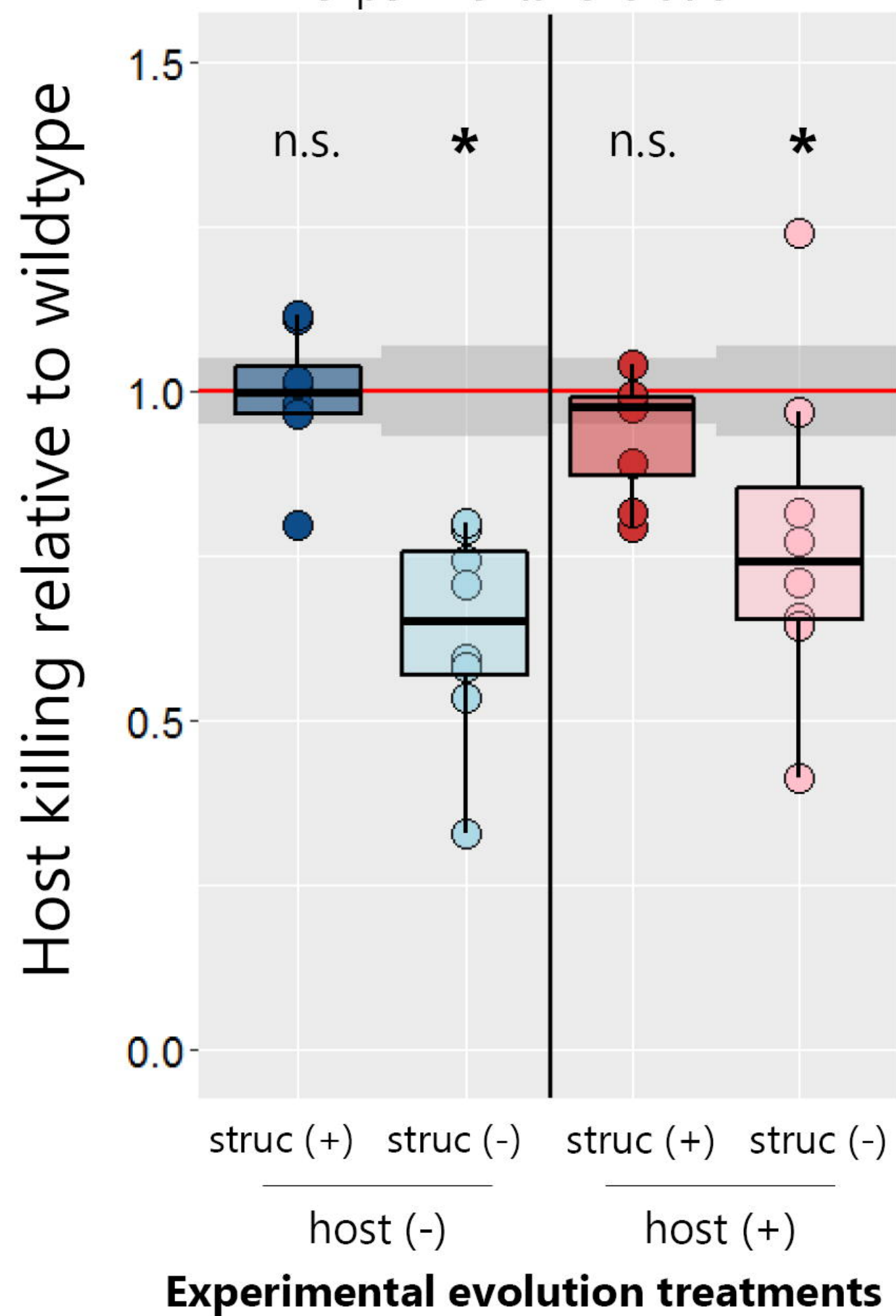
734 showed reduced protease production. The LasR regulator also has downstream effects on the
735 Rhl- and PQS quorum-sensing systems, which control pyocyanin production. Consistent with
736 this view, most clones with *lasR* mutations (93.8 %) showed decreased pyocyanin production.
737 Although the genotype-phenotype match was nearly perfect for mutated clones, a considerable
738 amount of clones also showed altered phenotypes without mutations in these two regulators,
739 suggesting that some of the phenotypic changes are caused by mutations in yet unidentified loci.

A

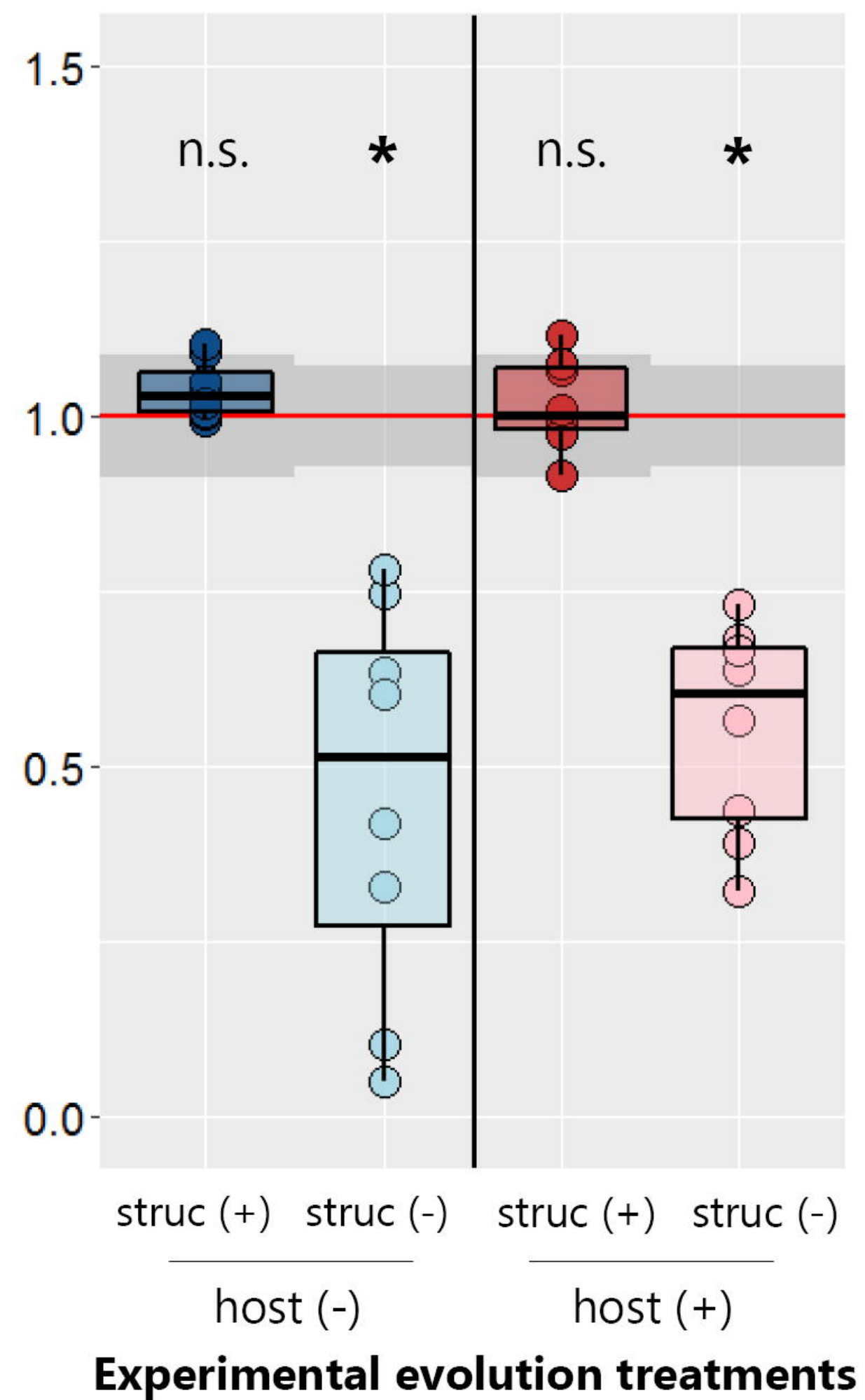
bioRxiv preprint doi: <https://doi.org/10.1101/250845>; this version posted June 18, 2018. The copyright holder for this preprint (which was not certified by peer review) is the author/funder, who has granted bioRxiv a license to display the preprint in perpetuity. It is made available under aCC-BY-NC-ND 4.0 International license.

**B**

Virulence tested in the spatial structure used during experimental evolution

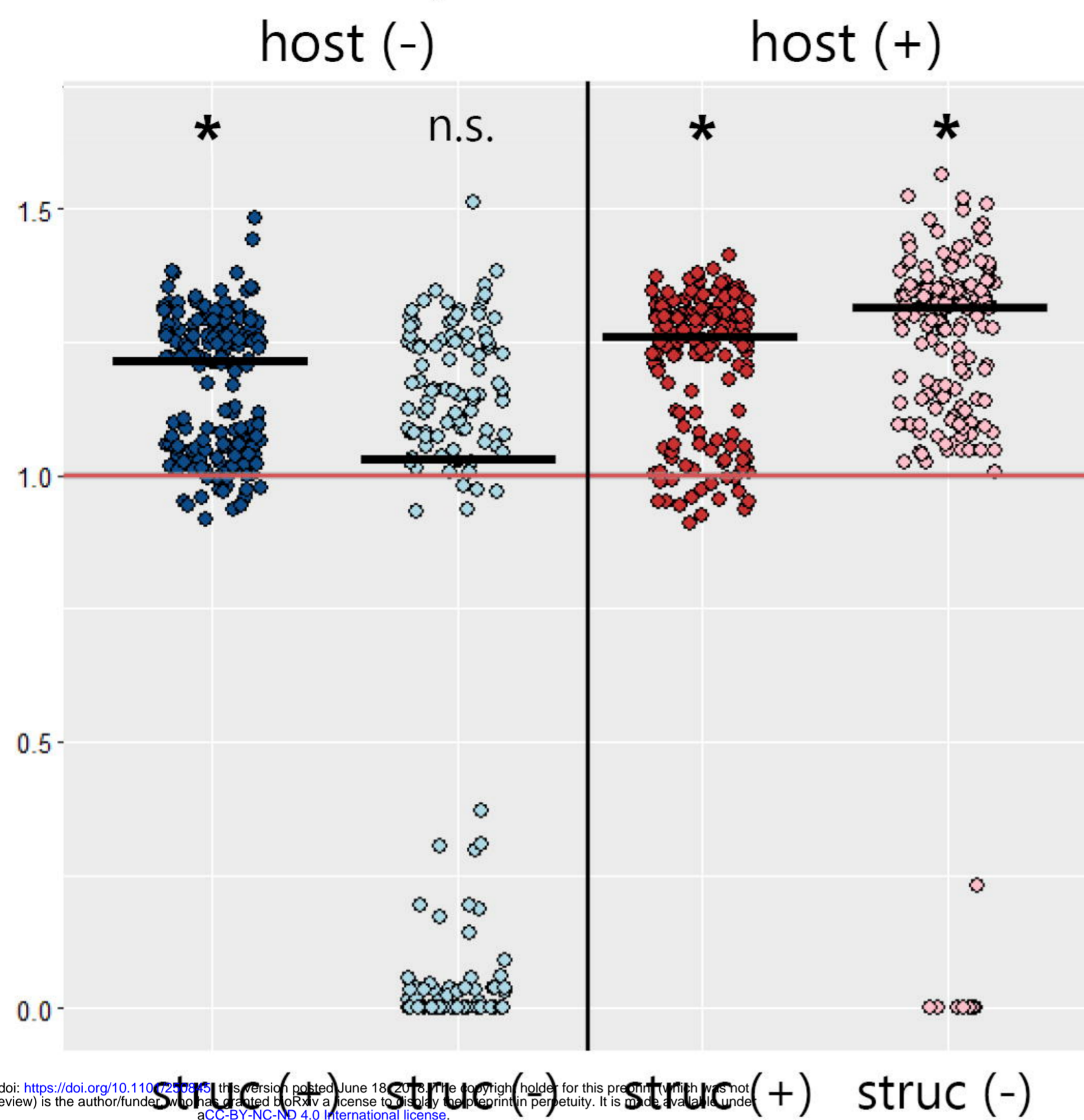
**C**

Virulence tested in the reciprocal spatial structure

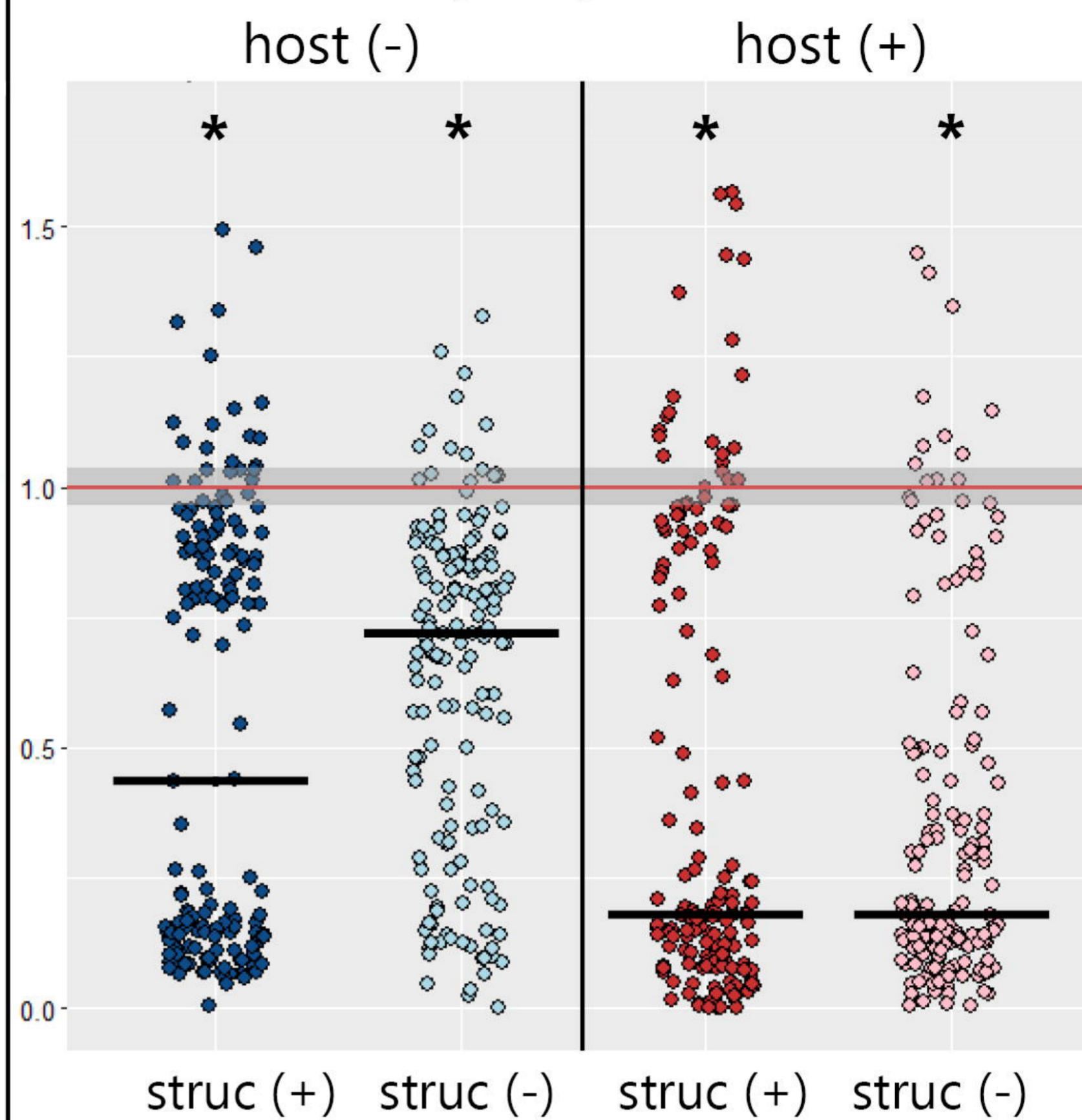


production relative to wildtype

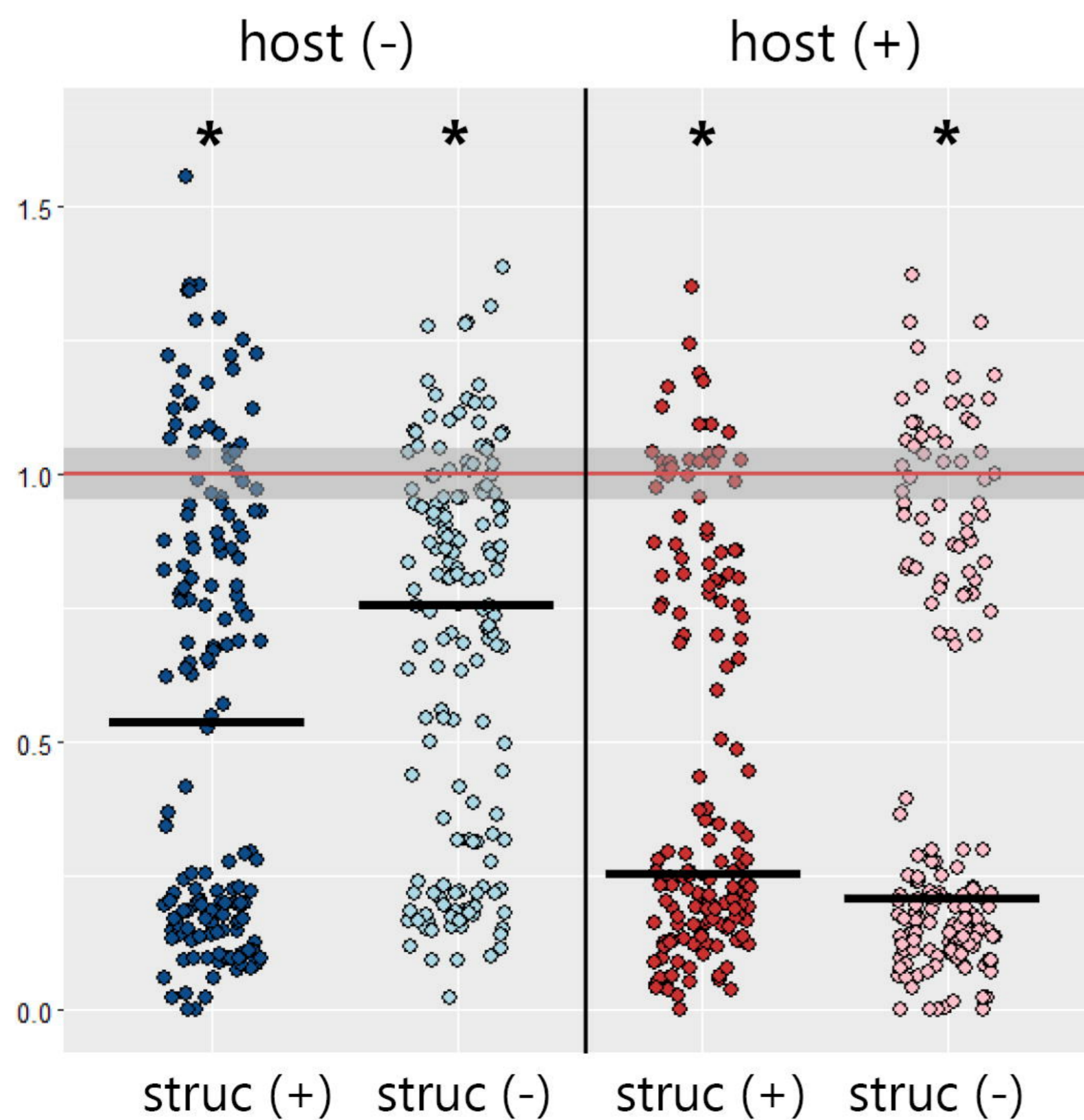
A Pyoverdine



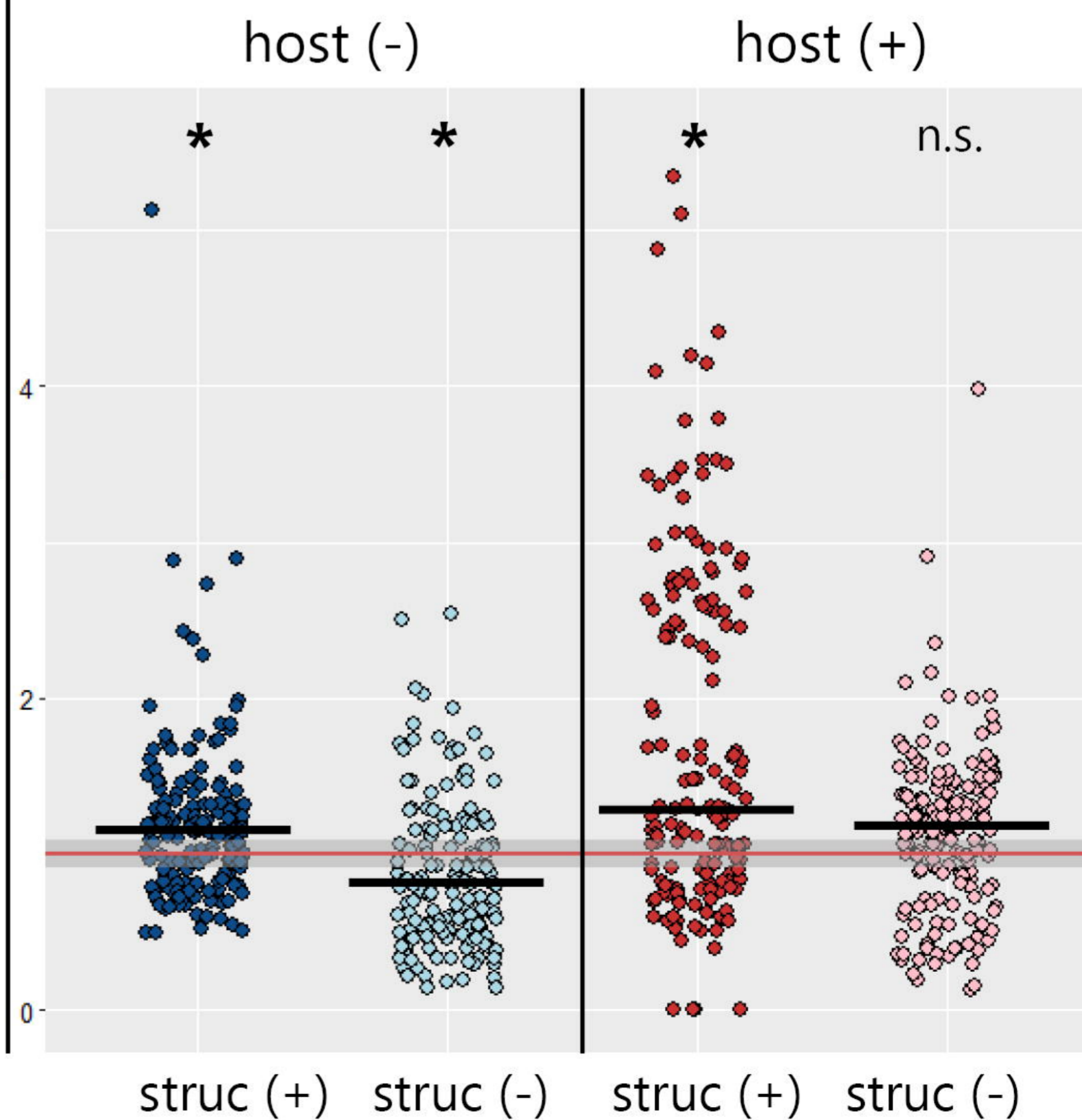
B Pyocyanin



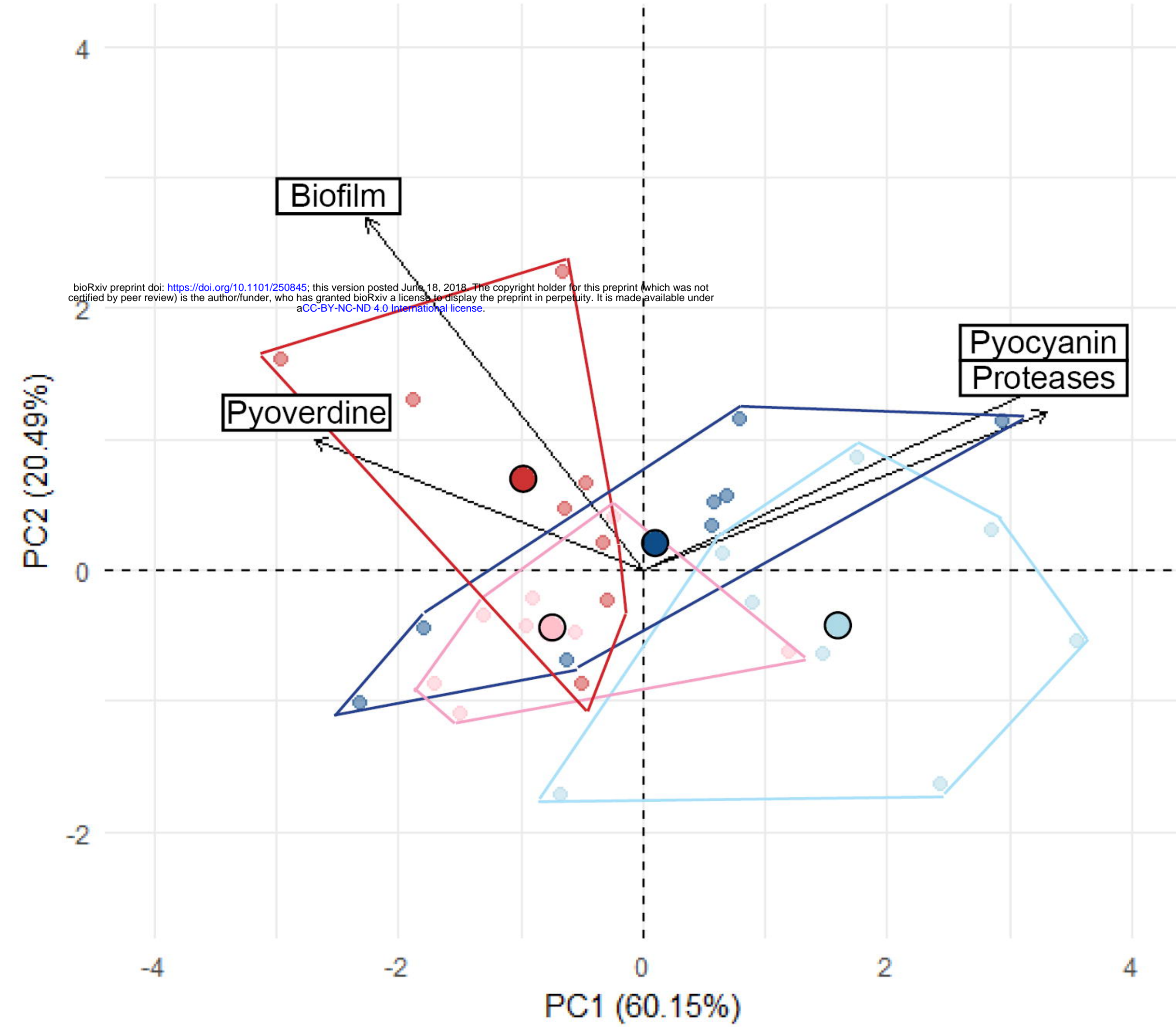
C Proteases



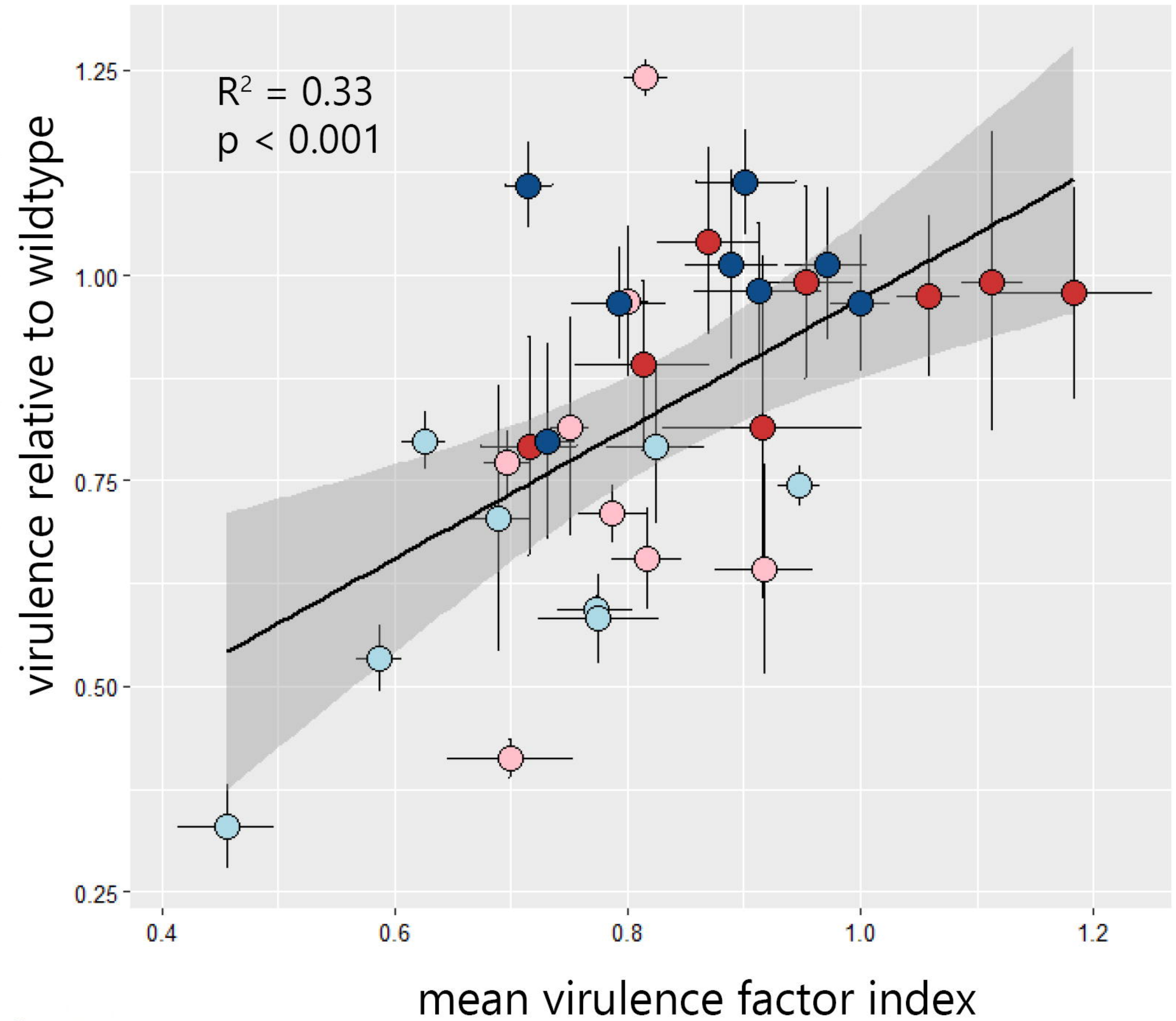
D Biofilm



A Principle component analysis



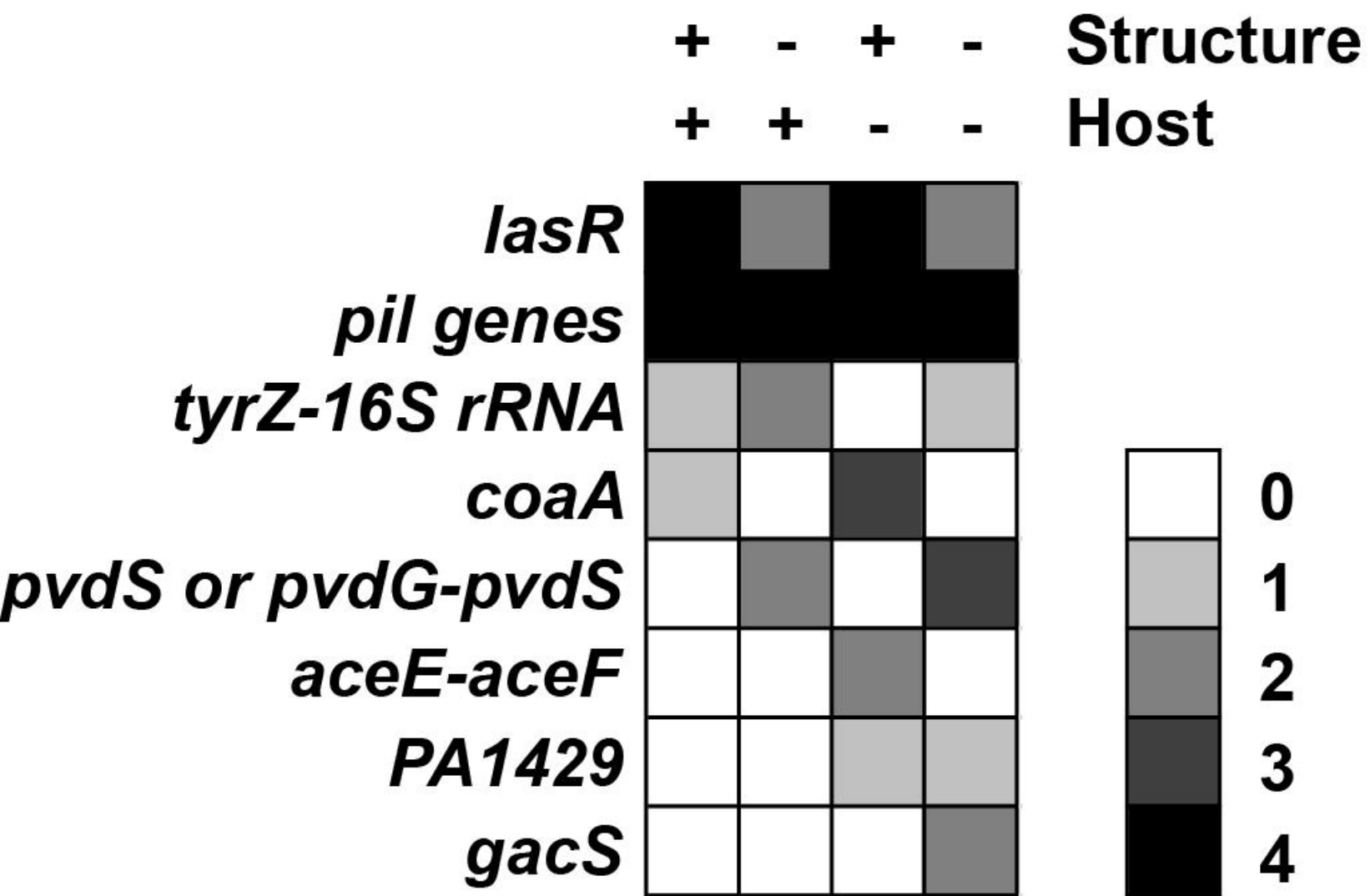
B



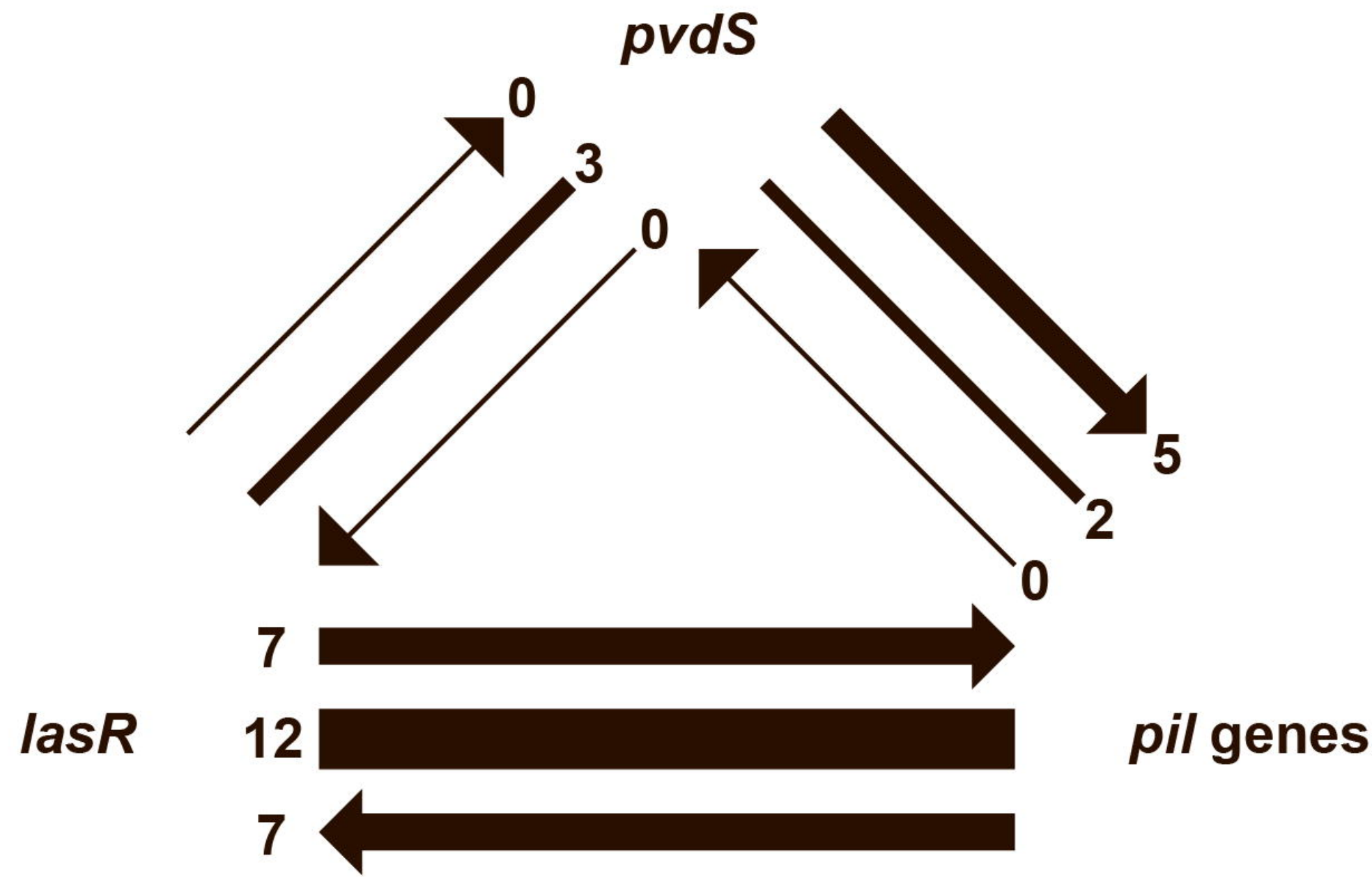
Environment



A Number of populations with mutation



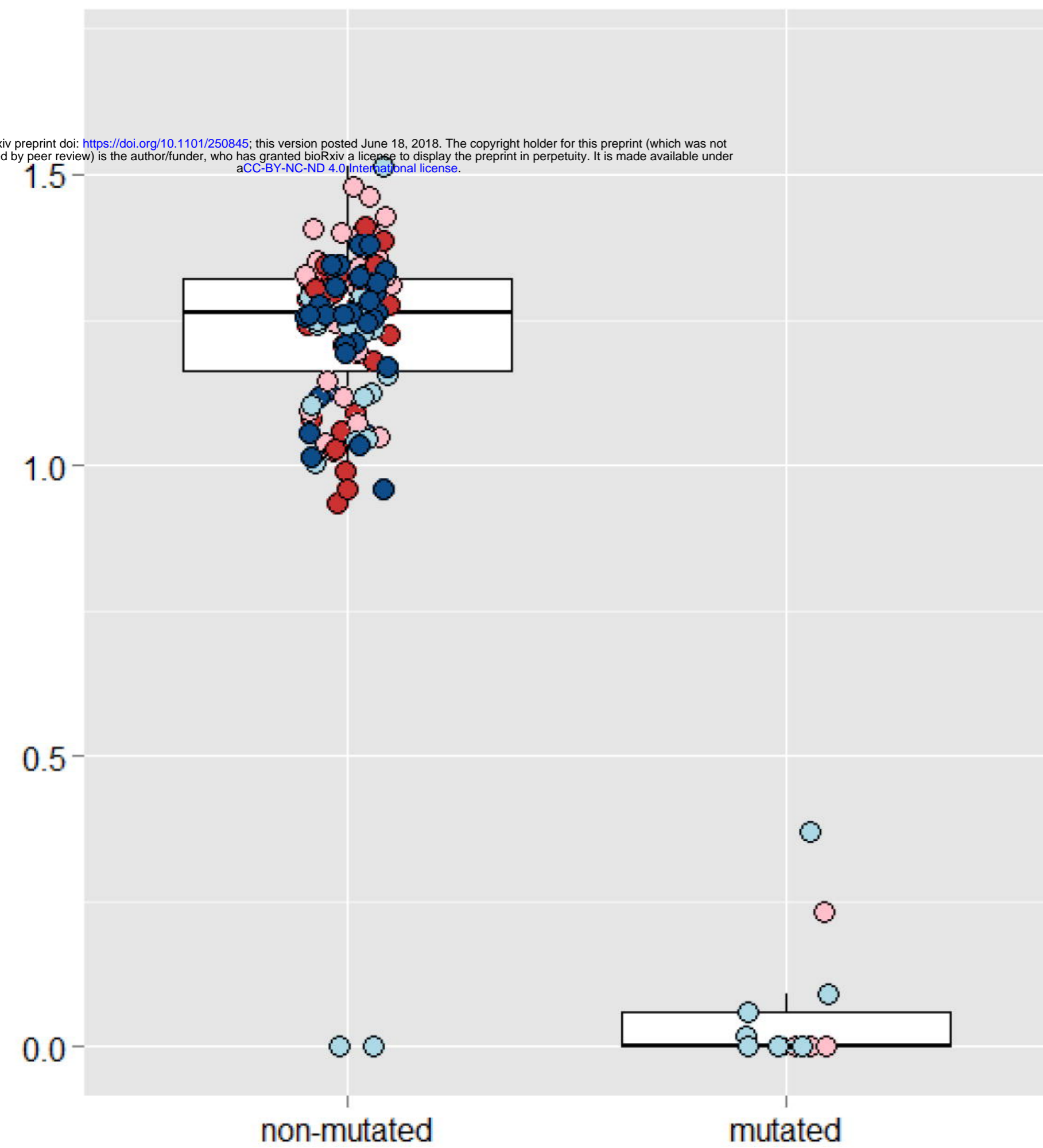
B Inferred order of pairwise mutations



production relative to wildtype

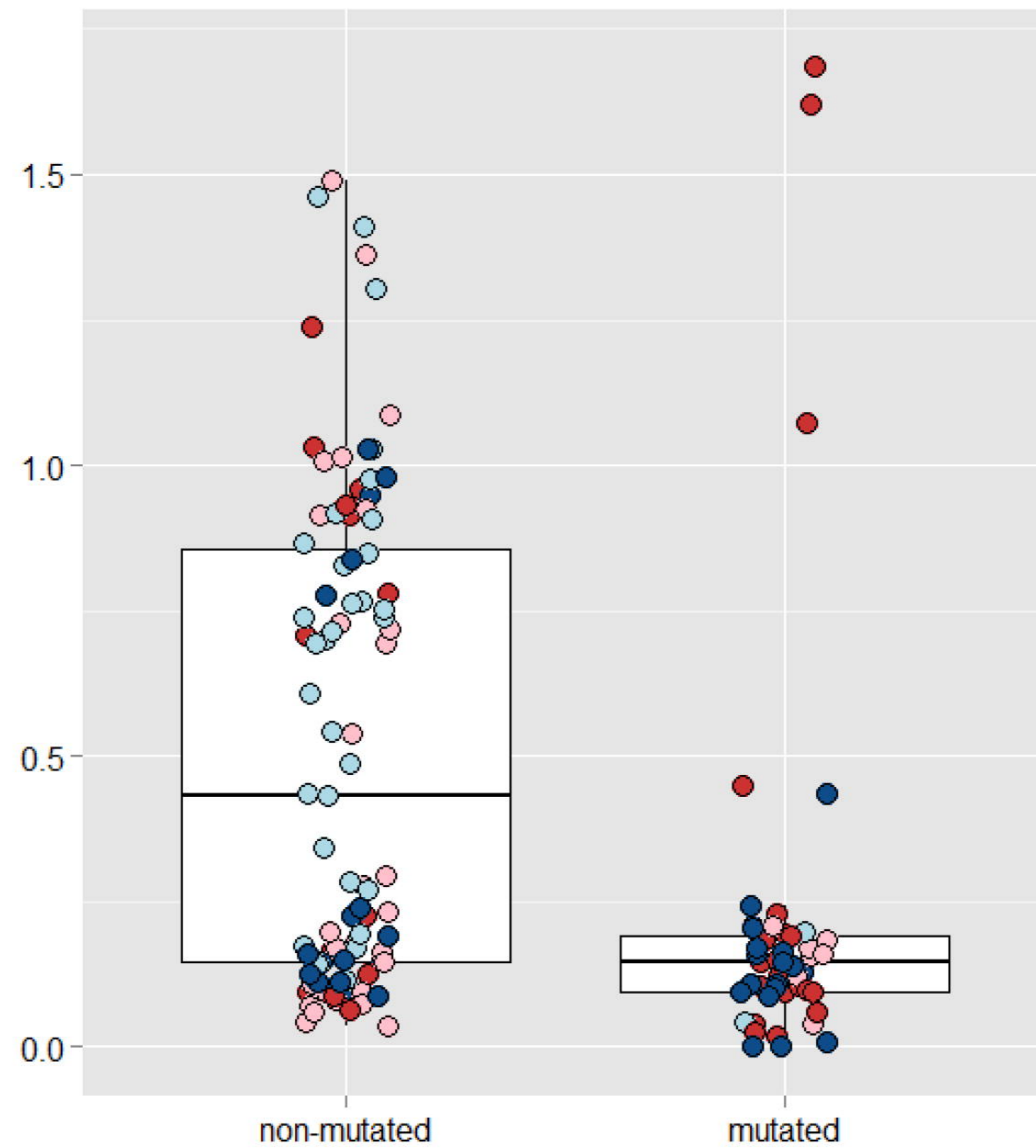
bioRxiv preprint doi: <https://doi.org/10.1101/250845>; this version posted June 18, 2018. The copyright holder for this preprint (which was not certified by peer review) is the author/funder, who has granted bioRxiv a license to display the preprint in perpetuity. It is made available under aCC-BY-NC-ND 4.0 International license.

A Pyoverdine



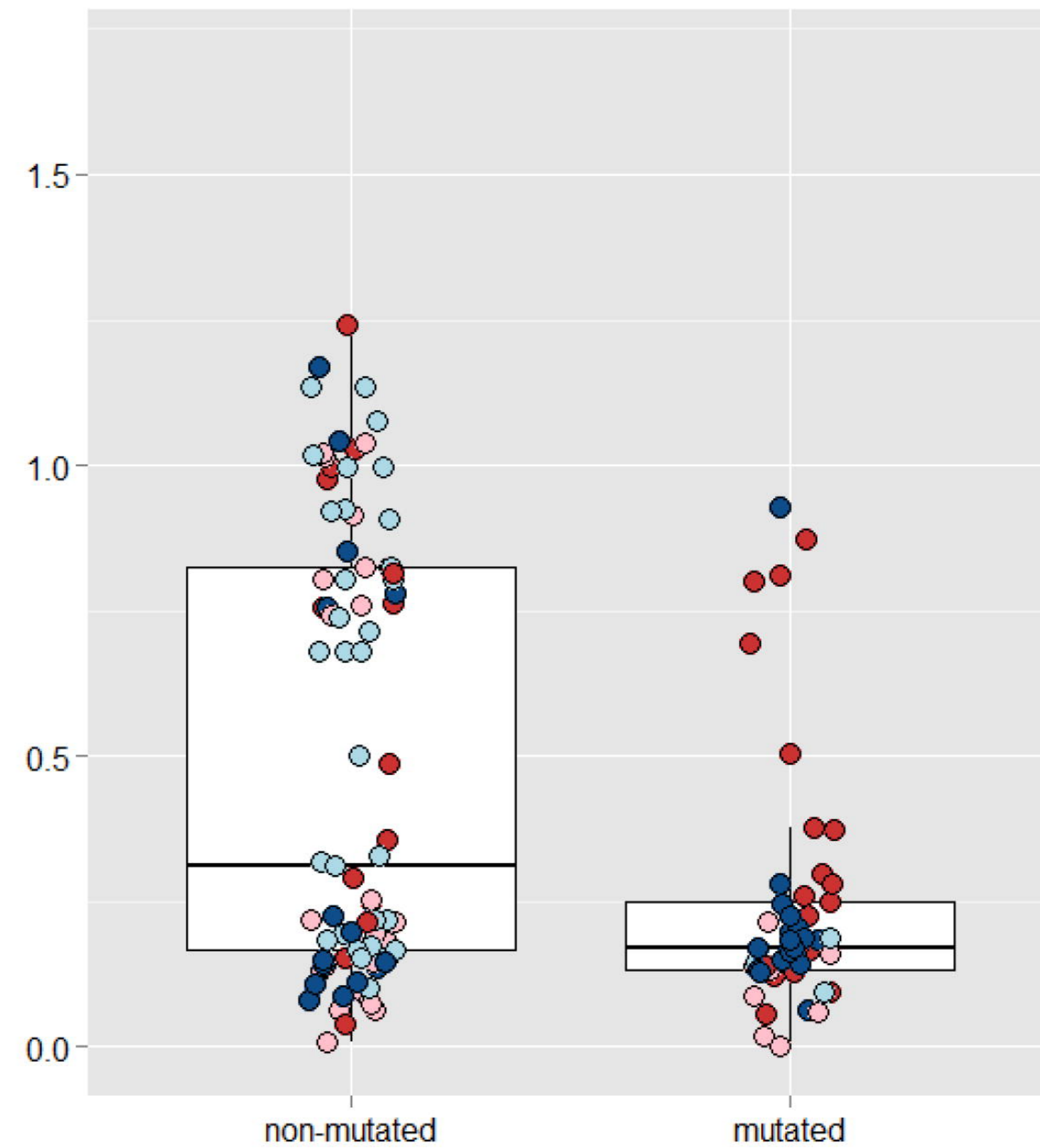
pvdS

B Pyocyanin



lasR

C Proteases



lasR